The New Keynesian Climate Model

Jean-Guillaume Sahuc, Frank Smets, Gauthier Vermandel

The New Keynesian Climate Model

Jean-Guillaume Sahuc
Frank Smets
Gauthier Vermandel

2025-1 Document de Travail/ Working Paper

EconomiX - UMR 7235 Bâtiment Maurice Allais
Université Paris Nanterre 200, Avenue de la République
92001 Nanterre Cedex

Site Web : economix.fr
Contact : secreteriat@economix.fr
Twitter : @EconomixU

THE NEW KEYNESIAN CLIMATE MODEL

JEAN-GUILLAUME SAHUC FRANK SMETS GAUTHIER VERMANDEL

ABSTRACT. Climate change confronts central banks with two inflationary challenges: *climate-flation* and *greenflation*. We investigate their implications for monetary policy by developing and estimating a tractable nonlinear New Keynesian Climate model featuring climate damages and mitigation policies for the global economy. We find that mitigation policies aligned with the Paris Agreement result in higher, more persistent inflation than laissez-faire policies. Central banks can attenuate this inflationary pressure by accounting for the rising natural rate of interest, at the cost of lower GDP during the transition. This short-term trade-off ensures long-term macroeconomic stability resulting from a net-zero emission world.

JEL: E32, E52, Q50, Q54.

Keywords: Climate change, inflation, monetary policy, E-DSGE model, Bayesian estimation, stochastic growth

J.-G. Sahuc: Banque de France, 31 rue Croix des Petits Champs, 75049 Paris, France, and University Paris-Nanterre (e-mail: jean-guillaume.sahuc@banque-france.fr). F. Smets: Bank for International Settlements, Centralbahnplatz 2, 4051 Basel, Switzerland, Ghent University and CEPR (frank.smets@ugent.be). G. Vermandel: CMAP, Ecole Polytechnique, Institut Polytechnique de Paris, Route de Saclay, Palaiseau ; University Paris-Dauphine & PSL, LEDA UMR CNRS 8007, Place du Maréchal de Lattre de Tassigny, 75016 Paris, France, and Banque de France, 31 rue Croix des Petits Champs, 75049 Paris, France (e-mail: gauthier@vermandel.fr). We thank Nicoletta Batini, Ghassane Benmir, Marco Del Negro, Simon Dietz, Francesca Diluiso, Stephie Fried, Lars Peter Hansen, John Hassler, Felix Kluber, Anton Nakov, Conny Olovsson, Maria Sole Pagliari, Evi Pappa, Philipp Pfeiffer, Ricardo Reis, Fabien Tripier, Rick van der Ploeg as well as participants in several workshops and conferences for helpful comments The views expressed in this paper are those of the authors and do not necessarily reflect the views of the Banque de France, the European Central Bank or the Eurosystem. Declarations of interest: none.

1. INTRODUCTION

As climate change accelerates, central banks worldwide are confronted with two emerging challenges to their price stability mandates. The first issue is *climateflation*, which refers to the inflationary effects resulting from climate-related events (extreme weather, natural disasters, resource scarcity) and their adverse effects on the economy's productivity. The second challenge is *greenflation*, which pertains to inflationary pressures stemming from the transition to a low-carbon economy, characterized by higher carbon taxes and abatement spending. While the first phenomenon can be characterized as an adverse supply shock, the second is a mixture of a positive cost-push shock and a positive demand shock. Central banks face a delicate balancing act in addressing both climateflation and greenflation and maintaining price stability, while supporting the real economy.

In this paper, we investigate these two phenomena and their implications for central bank policy-making. To this end, we develop and estimate a tractable nonlinear New Keynesian Climate (NKC) model for the world economy featuring climate change damage and mitigation policies. As illustrated in Galí (2015)'s textbook, the New Keynesian framework captures the interplay between aggregate demand and supply, highlighting the role of inflation, output, and monetary policy in shaping the overall economic landscape. By augmenting the traditional 3-equation model with elements that capture climate externalities and abatement costs, we aim to enrich our understanding of how climate change affects the economy. The tractability of this framework facilitates the analytical decomposition of the inflationary effects, including due to climateflation and greenflation.

Our first contribution is to bridge the gap between integrated assessment models (IAMs), developed to study carbon mitigation policies from a long-term perspective, and the New Keynesian dynamic stochastic general equilibrium models (DSGEs), which are usually dedicated to the analysis of economic fluctuations. Our New Keynesian Climate (NKC) model keeps the elegance and tractability of the textbook model by incorporating *(i)* a single additional endogenous variable (the stock of carbon), *(ii)* four exogenous trends (population, carbon intensity, abatement efficiency and technological) and, *(iii)* one exogenous carbon tax. Consequently, the model is reduced to the following four equations. The IS curve incorporates green investment spending to reduce carbon emission. The Phillips curve considers the economic damage from rising carbon stocks and the production cost from abatement efforts. The monetary policy rule links the nominal interest rate to the deviation of inflation from its

target and the output gap. Finally, the last equation is the law of motion that governs the accumulation of carbon dioxide emissions, which makes it depend on the current flow of production adjusted for abatement efforts. These equations form the basis for analyzing the impact of climate change on key macroeconomic variables and policy responses.

Our second contribution is to use a solution method that accounts for both *(i)* the structural change caused by rising carbon emissions and abatement spending and *(ii)* stochastic fluctuations due to exogenous shocks around the evolving economy. [1] Indeed, climate change and its associated mitigation policies have nonlinear and permanent effects on both the supply and demand sides of the economy and the natural real interest rate. [2] Therefore, the usual practice in monetary policy literature for analyzing the propagation of small shocks around a detrended steady state is not appropriate. Indeed, the accumulation of carbon stock leads to permanent shifts in the economy's long-term state, requiring alternative tractable solution methods that do not rely on a steady-state. Consequently, this paper introduces a refined version of the extended path solution method from Fair and Taylor (1983), designed to numerically capture both the high-frequency dynamics driven by shocks and the long-term transitional effects associated with technological changes and climate dynamics. This approach uses a perfect foresight solver to solve the long term path of the economy. In each period, agents are surprised by the realization of shocks but they still expect that in the future, shocks are zero on average, consistent with rational expectations. Second, an inversion filter is used to calculate the likelihood function. By recursively extracting the sequence of innovations through the inversion of observation equations, this filter has recently emerged as a computationally efficient method (Guerrieri and Iacoviello, 2017). Finally, using Bayesian techniques, as in Smets and Wouters (2003, 2007), we estimate the structural parameters using four global macroeconomic and climate-related time series from 1985Q1 to 2023Q2.

Our third contribution is to use the estimated model to quantitatively measure climateflation and greenflation, as well as the associated monetary policy responses, across different transition scenarios. Our framework differs from existing studies on greenflation (e.g., Del Negro et al., 2023; Nakov and Thomas, 2023; Olovsson and Vestin, 2023; Pappa et al., 2023),

[1] For a comprehensive discussion regarding the primary assumptions underlying economic climate change models and their associated solution methodologies, we refer to Fernández-Villaverde et al. (2024).

[2] In a climate damage function, the effect of cumulative carbon on production does not scale proportionally with the size of the economy, breaking the assumptions required for traditional detrending methods.

which primarily focus on partial transitions and fail to achieve a full net-zero transition. [3] In contrast, our framework provides a bridge between integrated assessment and New Keynesian models, enabling the examination of complete transitions from either a continuously warming planet or a state of net-zero emissions. The first scenario is a "laissez-faire" economy characterized by an increasing stock of carbon, that warms the planet and makes resources scarcer. The increasing damage to total factor productivity acts as a permanent negative supply shock that fuels inflation and drives output below its technological trend (Schnabel, 2022). The second scenario captures the "Paris-Agreement", which requires world governments to implement mitigation policies to reach net-zero carbon emissions by 2050. In our framework, this scenario takes the form of a linear increase in the carbon tax such that full abatement is reached in 2050. The rise in carbon tax forces firms to internalize the effects of their carbon emissions on aggregate productivity. In response, they reduce their emissions by increasing abatement expenditures, creating a demand-driven boom. We use these two scenarios *(i)* to explore the trade-offs between current abatement efforts and future damages, and *(ii)* to study their implications for natural output and real interest rate, inflation and monetary policy responses.

Our analysis highlights four major results. First, under the estimated monetary policy reaction function we find that the green transition under the Paris Agreement leads to higher and more persistent inflation than under a laissez-faire environmental policy. This conclusion remains robust across various alternative specifications of the model, including wage rigidities and investment adjustment costs. Second, we identify a crucial intertemporal trade-off for central banks: The short-term costs of the green transition, characterized by heightened dispersion in inflation and output, must be balanced against the long-term benefits of higher output and consumption. Postponing the transition intensifies the economic costs of climate damages, with output dispersion increasing by approximately 30% post-2050. Third, our results emphasize the necessity of integrating the evolving natural rate of interest into monetary policy rules. Static rules expressed as deviations from the steady state lead to an additional 1.5% annual inflation during the transition, whereas climate-adaptive Taylor rules

[3] Del Negro et al. (2023), Olovsson and Vestin (2023) and Pappa et al. (2023) do not address the inflationary consequences of climate-related damages and focus on a limited, short-term transition that fails to attain net-zero emissions. Conversely, Nakov and Thomas (2023) provide valuable insights by incorporating economic damages into their analysis, though they do not explore the potential inflationary implications. Moreover, their proposed framework only manages to reduce emissions by less than 50%, which falls short of a comprehensive abatement strategy.

that integrate the natural interest rate mitigate the inflationary effects of carbon taxes. Finally, we show that the social cost of carbon remains largely unaffected by price stickiness. [4] Although these rigidities slightly reduce consumption through the menu costs, they do so through quantitatively small wealth effects on the marginal utility of consumption. As a result, the social cost of carbon remains largely unaffected, reinforcing the case for ambitious climate policies comparable to those currently considered in flexible price contexts.

Our paper is related to the burgeoning literature that focuses on climate issues using microfounded structural models. Heutel (2012) was among the first to introduce carbon emissions into a quantitative real business cycle model. He assumed that emissions stem from production and adversely impact utility or have a negative impact on productivity and production. Recent contributions have extended these models in several directions, including *(i)* multisector aspects (Golosov et al., 2014), *(ii)* labor market frictions (Gibson and Heutel, 2023; Finkelstein Shapiro and Metcalf, 2023), *(iii)* endogenous entry (Annicchiarico et al., 2018; Finkelstein Shapiro and Metcalf, 2023), *(iv)* nominal rigidities and monetary policy (Annicchiarico and Di Dio, 2015, 2017; Carattini et al., 2023; Diluiso et al., 2021; Ferrari and Nispi Landi, 2024; Olovsson and Vestin, 2023; Coenen et al., 2024; Del Negro et al., 2023), *(v)* distributional implications of energy price shocks similar to those of carbon price shocks (Benmir and Roman, 2022; Auclert et al., 2023; Langot et al., 2023), and *(vi)* the asset pricing implications of carbon tax (Benmir et al., 2020). While these studies offer valuable insights into the role of green transition, they do not explicitly address the nonlinear dynamics of carbon accumulation, technology and demography and their permanent effects on the economy. In contrast, our framework captures both long-run trends in carbon emissions and macroeconomic variables, as in Jondeau et al. (2023), while also accounting for business cycle fluctuations driven by shocks. Moreover, our framework incorporates an estimation phase, allowing it to align closely with the observed data and produce macroeconomic outcomes based on statistical forecasts. This dual capability makes our framework particularly well suited for studying the effects of environmental policies over both short and long runs.

An emerging body of work, referred to as the greenflation literature, has quantitatively explored the inflationary impacts of green transition. Recent studies have contributed to this growing field by exploring various aspects of the interaction between monetary policy and climate change. For instance, Nakov and Thomas (2023), using a nonlinear New Keynesian

[4] The social cost of carbon has become a key metric in policy circles, representing the socially optimal price for emitting one ton of CO_2.

model with climate change externalities, analyzed how optimal monetary policy navigates the trade-off between price stability and climate objectives, highlighting how this balance depends on the (sub)optimality of green transition policies. Similarly, Olovsson and Vestin (2023), in a nonlinear two-sector model with price and wage rigidities, demonstrated that during a green transition, monetary policy is most effective when it focuses on core inflation and overlooks transitory increases in energy prices, leading to only a modest rise in inflation. Pappa et al. (2023), employing a small nonlinear open-economy model, investigated the role of energy efficiency and emphasize the importance of fiscal policy in supporting the transition. Finally, Del Negro et al. (2023) contributed to the literature by examining how production network structures influence the path of green transition. Their findings suggest that the presence of production networks amplifies the inflationary surge during the transition, driven by complementarities within the network that exacerbate the relative input price fluctuations. Our approach is distinct from the greenflation literature in several ways. First, we estimate a nonlinear model, aligning it more closely with data in the spirit of Smets and Wouters (2007). Second, unlike models relying on green-versus-brown substitution, our framework circumvents the limitations inherent in production functions based on constant elasticity of substitution (CES) aggregators (see Jo and Miftakhova, 2024, for a discussion on the unrealistic nature of the CES assumption), which cannot achieve net-zero emissions with a zero-brown sector. [5] As a result, such models are unable to simulate a complete transition scenario to net zero, such as those outlined in the Intergovernmental Panel on Climate Change reports. By contrast, our framework incorporates abatement curves from the Dynamic Integrated Climate-Economy model (Barrage and Nordhaus, 2024), enabling an analysis of transitions ranging from net-zero emissions to continued global warming. Importantly, our model is the first Integrated Assessment Model to include nominal rigidities, where expectations drive inflation dynamics, and monetary policy plays a key role in mitigating inflationary forces related to climate factors.

The remainder of this paper is organized as follows. Section 2 presents the micro-foundations of the NKC and its summary into four core equations. Section 3 presents the data transformation, and prior and posterior distributions. Section 4 presents the anatomy of the green

[5] Achieving this would require an infinite relative price ratio between brown and green inputs. These studies, therefore, limit their analysis to partial transition dynamics toward intermediate objectives, such as a 50 percent reduction in emissions by 2030. These frameworks cannot be classified as Integrated Assessment Models, as they do not capture the complete transition to net zero emissions.

transition and analyzes how climateflation and greenflation phenomena may affect the world economy by 2100. Section 5 discusses the implications of the green transition for the central bank. Section 6 examines the concept of social cost of carbon within our framework. Section 7 presents additional exercises to check the robustness of the analysis. Section 8 concludes.

2. The 4 equation New Keynesian climate (NKC) model

Our starting point is the textbook three equation New Keynesian model (Woodford, 2003, Galí, 2015), which includes an IS curve, a Phillips curve, and a Taylor-type rule. To this standard framework, we add climate dynamics by mixing Golosov et al. (2014) and Nordhaus (1992).

2.1. **Household sector.** The economy is populated by a mass l_t of ex-ante atomistic, identical, and infinitely lived households. This mass is time-varying and captures the upward trend of the population observed over the last 60 years. Formally, it is assumed that the population asymptotically converges to a long-run level $l_\infty > 0$, such as $l_t = l_{t-1}\left(l_\infty / l_{t-1}\right)^{\ell_g}$, with $\ell_g \in [0,1]$ being the geometric rate of convergence to l_∞. Each household indexed by $i \in [0, l_t]$ maximizes its sequence of present and future utility flows that depend positively on consumption $c_{i,t}$ and negatively on labor $n_{i,t}$:

$$\mathbb{E}_t \left\{ \sum_{s=0}^{\infty} \tilde{\beta}_{t,t+s} \varepsilon_{b,t+s} \left(\frac{c_{i,t+s}^{1-\sigma_c} - 1}{1-\sigma_c} - \psi_{t+s} \frac{n_{i,t+s}^{1+\sigma_n}}{1+\sigma_n} \right) \right\}, \tag{1}$$

where $\mathbb{E}_t$ denotes the expectation conditional on the information available at t, $\tilde{\beta}_{t,t+s}$ is the technological-neutral discount factor, [6] $\sigma_c > 0$ is the inverse of the intertemporal elasticity of substitution in consumption, $\sigma_n > 0$ is the inverse of the Frisch labor supply elasticity, and ψ_t is a scale variable pinning down hours worked in a balanced growth path. [7] In addition, $\varepsilon_{b,t}$ is a preference shock that captures unexpected changes in aggregate demand. It follows an AR(1) process: $\varepsilon_{b,t} = (1-\rho_b) + \rho_c \varepsilon_{b,t-1} + \eta_{b,t}$, with $\eta_{b,t} \sim \mathcal{N}(0, \sigma_b^2)$.

As in McKay et al. (2017), households are endowed with stochastic idiosyncratic employment status $\varsigma_{i,t} \in \{0,1\}$, with 0 indicating low productivity (denominated "type L" worker)

[6] The presence of a permanent increase in technology affects the Euler equation, and consequently the natural real interest rate and the monetary policy rule. To keep the framework tractable, we mute the effect of technology on the long-run equilibrium rate by imposing: $\tilde{\beta}_{t,t+s} = \beta(z_{t+s}/z_t)^{\sigma_c}$ with $\beta \in (0,1)$. Note that this assumption is standard in models featuring recursive utility functions such as Epstein-Zin for instance.

[7] Note that ψ_t must grow proportionally with the flow of current consumption. Thus, if z_t denotes the trend in per capita consumption, $\psi_t = \psi z_t^{1-\sigma_c}$, with ψ as a scale parameter.

and 1 high productivity (denominated "type H" worker). The level of productivity is drawn i.i.d. with probabilities $\Pr(\varsigma_{i,t} = 0) = \omega$ and $\Pr(\varsigma_{i,t} = 1) = 1 - \omega$. The sequence of real budget constraints for each type of households is as follows:

$$c_{i,t} + b_{i,t} + T^s_{i,t} = \frac{r_{t-1}}{\pi_t} b_{i,t-1} + \Pi_{i,t} + w_t n_{i,t} + \frac{T^e_{i,t}}{1-\omega}, \text{ if } \varsigma_{i,t} = 1, \tag{2}$$

$$c_{i,t} + b_{i,t} = \frac{r_{t-1}}{\pi_t} b_{i,t-1} + d_{i,t}, \text{ if } \varsigma_{i,t} = 0, \tag{3}$$

where variable $b_{i,t}$ is the one-period riskless bond, r_t is the gross nominal interest rate on bonds, $\pi_t = p_t / p_{t-1}$ is gross inflation with p_t being the price index, $\Pi_{i,t}$ are real dividend payments received from holding shares of firms, w_t is the aggregate real wage, and $T^e_{i,t}$ represents the revenues of the carbon tax redistributed through lum-sum transfers. Low-productivity households receive $d_{i,t}$ units of the consumption good as a transfer, and high-productivity households pay a tax of $T^s_{i,t} = \omega d_{i,t} / (1-\omega)$ to finance the transfer. This transfer is assumed to be time-varying, increasing proportionally to productivity z_t and environmental damages (represented by the function $\Phi(m_t)$ defined subsequently).

Thus, the Euler equation associated with the problem of household i of productivity type $q \in \{H, L\}$ is given by:

$$\varepsilon_{b,t} c^{-\sigma_c}_{i,q,t} \geq \mathbb{E}_t \left\{ \frac{\tilde{\beta}_{t,t+1} \varepsilon_{b,t+1} r_t}{\pi_{t+1}} \left((1-\omega) c^{-\sigma_c}_{i,H,t+1} + \omega c^{-\sigma_c}_{i,L,t+1} \right) \right\}, \tag{4}$$

where $c_{i,H,t}$ and $c_{i,L,t}$ denote consumption of high- and low-productive households, respectively.

2.2. **Business sector.** The business sector is characterized by final good producers who sell a homogeneous final good to households and the government. To produce, they buy and pack differentiated varieties produced by atomistic and infinitely lived intermediate goods firms that operate in a monopolistically competitive market. Intermediate goods firms contribute to climate change by emitting CO_2 as an unintended result of their production process.

2.2.1. *Final good sector.* At every point in time t, a perfectly competitive sector produces a final good Y_t by combining a continuum of intermediate goods $y_{j,t}$, $j \in [0, l_t]$, according to the technology $y_t = \left[l_t^{-1/\zeta} \int_0^{l_t} y_{j,t}^{\frac{\zeta-1}{\zeta}} \mathrm{d}j \right]^{\frac{\zeta}{\zeta-1}}$. The number of intermediate good firms owned by households is equal to the size of the population l_t. Parameter $\zeta > 1$ measures the substitutability across differentiated intermediate goods. Final good producing firms take

their output price, p_t, and their input prices, $p_{i,t}$, as given and beyond their control. Profit maximization implies the demand curve $y_{j,t} = l_t^{-1} \left(p_{j,t}/p_t\right)^{-\zeta} y_t$, from which we deduce the relationship between the price of the final good and the prices of intermediate goods $p_t \equiv \left[l_t^{-1} \int_0^{l_t} {p_{j,t}}^{1-\zeta} \mathrm{d}j\right]^{\frac{1}{1-\zeta}}$.

2.2.2. *Intermediate goods sector.* Intermediate good j is produced by a monopolistic firm using the following production function:

$$y_{j,t} = \Gamma_t l_t^{1-\alpha} \left(n_{j,t}^d\right)^{\alpha}, \tag{5}$$

where Γ_t is the total factor productivity (TFP) that affects labor demand $n_{j,t}^d$, and $\alpha \in [0,1]$ indicates labor intensity.

The TFP is actually determined by two components:

$$\Gamma_t = z_t \Phi\left(m_t\right), \tag{6}$$

where z_t is the deterministic component of productivity and $\Phi(m_t)$ is a damage function that represents the impact of climate change on the production process. The deterministic component of TFP follows the process $z_t = z_{t-1}(1 + g_{z,t})$, where $g_{z,t} = g_{z,t-1}\left(1 - \delta_z\right)$ is the productivity growth rate and δ_z is the rate of decline in productivity. This formulation indicates that productivity growth has decreased over time by a factor δ_z to match the observed slowdown in economic growth per capita over the last century.

Finally, following Golosov et al. (2014), we assume an exponential damage function: [8]

$$\Phi(m_t) = \exp(-\gamma(m_t - m_{1750}))$$

where $m_t - m_{1750}$ is the excess carbon in the atmosphere net of its (natural) removal, with m_{1750} representing the stock of carbon in the preindustrial era. The atmospheric loading of CO_2 (in gigatons of CO_2) is given by:

$$m_t = m_{t-1} + \xi_m e_t, \tag{7}$$

where e_t denotes the anthropogenic carbon emissions in t, and $\xi_m \geq 0$ is the atmospheric retention ratio. Note that the carbon stock does not depreciate consistently with new evidence regarding the transient climate response to cumulative emissions of carbon dioxide (TCRE).

[8] This function approximates the damage function generally used in the DICE literature, which depends on atmospheric temperature.

A firm's CO_2 emissions stemming from its production process are denoted by $e_{i,t}$. Because they are subject to carbon tax $\tau_{e,t}$, which aims to internalize the social cost of carbon emissions, the firm is incentivized to reduce its impact by investing in emission abatement technology. The abatement effort of the firm yields a reduction by $\mu_{i,t}$ (in %) in its CO_2 emissions. A firm's emissions take the following form:

$$e_{j,t} = \sigma_t \left(1 - \mu_{j,t}\right) y_{j,t} \varepsilon_{e,t},$$

where σ_t denotes aggregate carbon intensity in the production sector. Its law of motion is $\sigma_t = \sigma_{t-1}(1 - g_{\sigma,t})$, where $g_{\sigma,t}$ captures the possible changes in the decrease in the carbon decoupling rate. These changes follow $g_{\sigma,t} = (1 - \delta_\sigma)\, g_{\sigma,t-1}$, where $\delta_\sigma \in [0, 1]$ is the rate of the decline in the trend. This trend matches the decline in the emission-to-GDP ratio observed over the past 60 years. Finally, a firm's carbon intensity can be temporarily affected by an aggregate exogenous emissions shock, $\varepsilon_{e,t} = (1 - \rho_e) + \rho_e \varepsilon_{e,t-1} + \eta_{e,t}$, with $\eta_{e,t} \sim N(0, \sigma_e^2)$, which captures the cyclical changes in the emissions-to-output ratio. An increase in $\varepsilon_{e,t}$ induces a cyclical increase in the carbon intensity in the production sector.

In practice, firms have three main possibilities to reduce carbon emissions. They may (i) substitute carbon-intensive technologies with low-carbon technologies; (ii) invest in energy-saving technologies; or (iii) purchase carbon sequestration. Much of the recent work on greenflation has solely focused on substitutions. [9] To capture all those three kinds of abatement actions, we introduce an abatement cost from Barrage and Nordhaus (2024). Each abatement action maps a marginal cost of reduction to a corresponding quantity of carbon abated. As the carbon price increases, a larger proportion of emissions is mitigated. This abatement cost function is particularly convenient, as it consolidates all forms of mitigation efforts into a simplified representation within a one-good, one-sector economy. The cost of abatement is given by:

$$\mathcal{C}^a_{j,t} = \theta_{1,t} \mu^{\theta_2}_{j,t} y_{j,t}, \tag{8}$$

where $\theta_{1,t} = (p_b/\theta_2)(1 - \delta_{pb})^{t-t_0}\sigma_t$ is the time-varying level of the abatement cost, $p_b > 0$ is a parameter determining the initial cost of abatement and $0 < \delta_{pb} < 1$ captures technological

[9] For instance, Olovsson and Vestin (2023); Nakov and Thomas (2023) analyze the effects of substituting two types of energy to achieve reductions in carbon emissions through CES energy aggregation. In contrast, Del Negro et al. (2023) generalize this approach to encompass the entire set of products within input-output tables. These studies, however, focus on only one type of abatement action related to input-output substitution. Our approach, inherited from the DICE model, incorporates all types of CO_2 mitigation actions in a highly stylized manner.

progress, which lowers the cost of abatement by a factor δ_{pb} each year. The literature on directed technological change typically endogenizes the rate of decline in green technologies, encapsulated in the parameter $\theta_{1,t}$. Finally, $\theta_2 > 0$ represents the curvature of the abatement cost function, which typically exhibits increasing returns in IAM literature.

Intermediate goods producers solve the typical two-stage problem. In the first stage, when input price w_t is taken as given, firms seek to maximize their one-period profits:

$$\max_{\{y_{j,t},\mu_{j,t}\}} mc_{j,t}y_{j,t} - w_t\left(\frac{y_{j,t}}{\Gamma_t}\right)^{1/\alpha} - \mathcal{C}^a_{j,t} - \tau_{e,t}\sigma_t\left(1-\mu_{j,t}\right)y_{j,t}\varepsilon_{e,t} \tag{9}$$

where $mc_{i,t}$ denotes the real marginal cost of producing one additional good.

In the second stage, firms decide their selling prices under the Rotemberg price setting. The Rotemberg price adjustment cost is given by:

$$\mathcal{C}^p_{j,t} = \frac{\kappa}{2}\left(\frac{p_{j,t}}{p_{j,t-1}} - \pi^\star_t\right)^2 \frac{y_t}{l_t} \tag{10}$$

where $\kappa > 0$ is the price stickiness parameter, y_t/l_t is the average market share per firm, and $\pi^\star_t$ is the gross inflation target, which follows a deterministic process (Ireland, 2007, Fève et al., 2010, Del Negro et al., 2015):

$$\pi^\star_t = \delta_{\pi^\star}\pi + (1-\delta_{\pi^\star})\pi^\star_{t-1}, \tag{11}$$

where $\delta_{\pi^\star}$ is the convergence rate, which reflects the slow pace at which monetary authorities adjusted their inflation target, and π is steady-state gross inflation. This trend reflects the significant decline in inflation and nominal interest rates observed globally in our sample starting in the 1980s, which we attribute to the gradual adoption of inflation-targeting regimes by central banks, leading to a structural reduction in inflation rates.

In New Keynesian models, announced policies such as climate policy lead to implausibly large effects in present value terms (e.g., the forward guidance puzzle discussed in Del Negro et al., 2023). To attenuate the expectation channel of inflation, an exogenous exit shock is introduced, consistent with empirical evidence on the survival rate of firms across time (OECD, 2017). As in Bilbiie et al. (2012), we assume a "death" shock, which occurs with probability $\vartheta \in (0,1)$ in every period. This means that each firm's profit is subject to an idiosyncratic

shock $\omega_{j,t}$ that takes the value 0 for the fraction of firms exiting the market. Thus, the problem faced by firms can be expressed as follows:

$$\max_{\{p_{j,t}\}} \mathbb{E}_t \left\{ \sum_{s=0}^{\infty} \beta^s \omega_{j,t+s} \left(y_{j,t+s} \frac{p_{j,t+s}}{p_{t+s}} - \varepsilon_{p,t+s} mc_{t+s} y_{j,t+s} - \mathcal{C}^p_{j,t+s} \right) \right\}, \tag{12}$$

subject to demand $y_{j,t} = l_t^{-1} \left(p_{j,t}/p_t \right)^{-\zeta} y_t$. $\varepsilon_{p,t}$ is a cost-push shock that follows an AR(1) process: $\varepsilon_{p,t} = (1-\rho_p) + \rho_p \varepsilon_{p,t-1} + \eta_{p,t}$, where $\eta_{p,t} \sim \mathcal{N}(0, \sigma_p^2)$.

Because all intermediate goods firms face an identical profit maximization problem, they choose the same price $p_{j,t} = p_t$. In a symmetric equilibrium, where the expected survival rate rate from t to $t+s$ is given by $(1-\vartheta)^s$, the optimal pricing rule implies:

$$\kappa \left(\pi_t - \pi_t^\star \right) \pi_t = (1-\vartheta)\beta\kappa \mathbb{E}_t \left\{ \left(\pi_{t+1} - \pi_{t+1}^\star \right) \pi_{t+1} \frac{y_{t+1}}{y_t} \frac{l_t}{l_{t+1}} \right\} + \zeta \varepsilon_{p,t} mc_t + (1-\zeta). \tag{13}$$

The above equation is the New Keynesian Phillips curve, which relates current inflation to the discounted sum of the marginal costs.

2.3. **Public sector.** The government issues short-term bonds, collects revenue from the carbon tax and redistributes it entirely to households on a lump-sum basis:

$$\int_0^{l_t} b_{i,t} \mathrm{d}i + + \tau_{e,t} \int_0^{l_t} e_{j,t} \mathrm{d}j = \frac{r_{t-1}}{\pi_t} \int_0^{l_t} b_{i,t-1} \mathrm{d}i + \int_0^{l_t} \Pr\left(z_{i,t} = 1\right) T^e_{i,t} \mathrm{d}i. \tag{14}$$

The monetary policy authority follows a Taylor-type rule by gradually adjusting the nominal interest rate in response to *(i)* the inflation gap and *(ii)* the output gap:

$$\frac{r_t}{r} = \left(\frac{r_{t-1}}{r} \right)^\rho \left[\left(\frac{\pi_t^\star}{\pi} \right) \left(\frac{\pi_t}{\pi_t^\star} \right)^{\phi_\pi} \left(\frac{y_t}{y_t^\star} \right)^{\phi_y} \right]^{1-\rho} \varepsilon_{r,t}, \tag{15}$$

where r is the long-run nominal interest rate and $y_t^\star$ is natural output, defined as the output that would prevail in imperfectly competitive markets but with flexible price. The parameters ρ_r, ϕ_π, ϕ_y capture the degree of interest-rate smoothing, and the responsiveness of the policy rate to the inflation and output gap, respectively. Finally, $\varepsilon_{r,t}$ is a monetary policy shock that follows the process: $\varepsilon_{r,t} = (1-\rho_r) + \rho_r \varepsilon_{r,t-1} + \eta_{r,t}$, with $\eta_{r,t} \sim N(0, \sigma_r^2)$,

2.4. **Aggregation.** First, we aggregate consumption for the two types of households:

$$l_t c_t = \int_0^{l_t} \Pr\left(z_{i,t} = 0\right) c_{L,t} \mathrm{d}i + \int_0^{l_t} \Pr\left(z_{i,t} = 1\right) c_{H,t} \mathrm{d}i, \tag{16}$$

It leads to:

$$c_t = \omega c_{L,t} + (1-\omega)\, c_{H,t}. \tag{17}$$

It is assumed that bonds ae in zero net supply:

$$\int_0^{l_t} b_{i,t} \mathrm{d}i = 0. \tag{18}$$

As discussed by McKay et al. (2017), as long as $c_{L,t} < c_{H,t}$, the Euler equation for the low productive worker does not bind to equality as the right-hand side will always be lower than the left-hand side. Therefore, let $\lambda_t = \varepsilon_{b,t} c_{H,t}^{-\sigma_c} = \varepsilon_{b,t} \left(\frac{c_t - \omega d_t}{1-\omega}\right)^{-\sigma_c}$ denote the marginal utility of consumption of highly productive households, the *aggregate* Euler equation is as follows:

$$\lambda_t = \mathbb{E}_t \left\{ \frac{\tilde{\beta}_{t,t+1} r_t}{\pi_{t+1}} \left((1-\omega)\lambda_{t+1} + \omega \varepsilon_{b,t+1} d_t^{-\sigma_c} \right) \right\}. \tag{19}$$

In contrast, the general equilibrium for hours worked reads as:

$$(1-\omega)\, n_t = n_t^d. \tag{20}$$

Finally, the resource constraint is given by:

$$y_t = l_t c_t + \frac{\kappa}{2} (\pi_t - \pi_t^\star)^2 y_t + \theta_{1,t} \mu_t^{\theta_2} y_t + \vartheta \Pi_t. \tag{21}$$

where Π_t is the profits that is consumed by the fraction of firms ϑ exiting the market.

2.5. **Final System.** The system can be summarized by the following set of four core equations that determine *(i)* the detrended GDP ($\tilde{y}_t = y_t/(l_t z_t)$), *(ii)* the nominal interest rate (r_t), *(iii)* the inflation rate (π_t) and *(iv)* the excess carbon in the atmosphere net of its natural level ($\tilde{m}_t = m_t - m_{1750}$).

The 4 Equation New Keynesian Climate Model:

(1) <u>*IS curve:*</u>

$$\left(\frac{x_t \tilde{y}_t - \omega \tilde{d}_t}{1-\omega}\right)^{-\sigma_c} = \beta \mathbb{E}_t \left\{ \frac{\varepsilon_{b,t+1}}{\epsilon_{b,t}} \frac{r_t}{\pi_{t+1}} \left((1-\omega) \left(\frac{x_{t+1}\tilde{y}_{t+1} - \omega \tilde{d}_t}{1-\omega} \right)^{-\sigma_c} + \omega \tilde{d}_t{}^{-\sigma_c} \right) \right\},$$

where $x_t = 1 - (1-\vartheta)\frac{\kappa}{2}(\pi_t - \pi_t^\star)^2 - \theta_{1,t} \tilde{\tau}_{e,t}^{\theta_2/(\theta_2-1)} - \vartheta(1 - \varepsilon_{p,t} m c_t)$
and $\tilde{d}_t = d\Phi(\tilde{m}_t)$

(2) *Phillips curve:*

$$(\pi_t - \pi_t^\star)\,\pi_t = (1-\vartheta)\beta\mathbb{E}_t\left\{(1+g_{z,t+1})\,\frac{\tilde{y}_{t+1}}{\tilde{y}_t}\,(\pi_{t+1}-\pi_{t+1}^\star)\,\pi_{t+1}\right\} + \frac{\zeta}{\kappa}\varepsilon_{p,t}mc_t + \frac{1-\zeta}{\kappa}$$

$$\text{where } mc_t = \frac{\psi}{(1-\omega)^{\sigma_c+\sigma_n}}\frac{\left(x_t\tilde{y}_t-\omega\tilde{d}_t\right)^{\sigma_c}\tilde{y}_t^{(1+\sigma_n)/\alpha-1}}{\Phi(\tilde{m}_t)^{(1+\sigma_n)/\alpha}} + \theta_{1,t}\tilde{\tau}_{e,t}\left[\theta_2+(1-\theta_2)\,\tilde{\tau}_{e,t}^{\frac{1}{\theta_2-1}}\right]$$

(3) *Monetary policy rule:*

$$\frac{r_t}{r} = \left(\frac{r_{t-1}}{r}\right)^\rho\left[\left(\frac{\pi_t^\star}{\pi}\right)\left(\frac{\pi_t}{\pi_t^\star}\right)^{\phi_\pi}\left(\frac{\tilde{y}_t}{\tilde{y}_t^\star}\right)^{\phi_y}\right]^{1-\rho}\varepsilon_{r,t},$$

(4) *Pollution stock dynamics:*

$$\tilde{m}_t - \tilde{m}_{t-1} = \xi_m\sigma_t\left(1-\tilde{\tau}_{e,t}^{\frac{1}{\theta_2-1}}\right)z_t l_t\tilde{y}_t\varepsilon_{e,t}.$$

In addition, the model comprises five exogenous trends $\{z_t, \theta_{1,t}, l_t, \sigma_t, \pi_t^\star\}$ and four AR(1) shocks $\{\varepsilon_{b,t}, \varepsilon_{p,t}, \varepsilon_{r,t}, \varepsilon_{e,t}\}$. [10]

3. Bayesian inference

In this section, we estimate the model using Bayesian methods (see An and Schorfheide, 2007, for an overview). The posterior distribution associated with the vector of observable variables is computed numerically using the Monte Carlo Markov Chain sampling approach. Specifically, we rely on the Metropolis-Hastings algorithm to obtain a random draw of size 20,000 from the posterior distribution of the parameters (eight parallel chains simultaneously draw 2,500 iterations, with a common jump scale parameter to match an acceptance rate of approximately 30%). First, we describe how the nonlinear model with trends is solved. We then discuss the data set together with our choice of priors and comment on the posterior distribution of the structural parameters.

3.1. Numerical solution method with stochastic growth.

We consider the *extended path solution method* from Fair and Taylor (1983) and Adjemian and Juillard (2014) to measure the nonlinear effects of environmental constraints on growth accurately. Briefly, the extended path approach uses a perfect foresight solver to obtain endogenous variables that are path consistent with the model's equations. In each period, agents are surprised by the realization of shocks, but still expect that in the future, shocks are zero on average (consistent with

[10] See Appendix A for the complete set of equations that incorporates the shock processes and trends.

rational expectations). The advantage of this method is that it provides an accurate and fast solution while considering all the nonlinearities of the model. [11] The drawback of this approach is that Jensen's inequality binds to equality, meaning that the nonlinear uncertainty stemming from future shocks is neglected. Note that this drawback also applies to typical linearized DSGE models, such as Smets and Wouters (2007).

Taking nonlinear models to the data is a challenge, as nonlinear filters, which are required to form the likelihood function, are computationally expensive. The inversion filter is a computationally-inexpensive alternative (e.g., Guerrieri and Iacoviello, 2017, Atkinson et al., 2020). Initially pioneered by Fair and Taylor (1983), this filter recursively extracts the sequence of innovations by inverting the observation equation for a given set of initial conditions. Unlike other filters (e.g. Kalman or particle filters), the inversion filter relies on an analytic characterization of the likelihood function. [12] The inversion filter uses the perfect foresight solution proposed by Juillard (1996) embedded into Dynare (Adjemian et al., 2024). The standard approach is to compute the dynamics of the variables given the current and future shocks. In the extended path context, the inversion filter *(i)* substitutes current shocks and some endogenous variables when applying the perfect foresight solution and *(ii)* computes current shocks and nonobservable variable paths given the set of observable variables. Finally, we use the Metropolis-Hastings algorithm as a sampler to draw from the parameter uncertainty. [13]

3.2. **Data description.** The model is estimated using quarterly worldwide data from 1985Q1 to 2023Q2. Because time series are not available on a quarterly basis, some transformations are necessary. First, the annual GDP in constant 2015 US$ is obtained from the *World Bank* (`https://data.worldbank.org/indicator/NY.GDP.MKTP.KD`), and is converted on a quarterly basis using the time disaggregation method of Chow and Lin (1971) using real quarterly GDP for total OECD countries from the *OECD Economic Outlook* database (`https://data.oecd.org/gdp/quarterly-gdp.htm`). [14] Quarterly headline inflation (`https:`

[11] Appendix B provides additional details on the general representation of the perfect foresight algorithm in the presence of extended path, and the underlying statistical model to estimate forward looking models with structural changes.

[12] For a presentation of alternative filters to calculate the likelihood function, see Fernández-Villaverde et al. (2016). See also Cuba-Borda et al. (2019) and Atkinson et al. (2020) for details on the relative gains of the inversion filter

[13] All our code is provided as a toolbox that extends the standard Dynare package Adjemian et al. (2024) and is available upon request.

[14] This temporal disaggregation technique uses a statistical relationship between low-frequency data and higher-frequency indicator variables. First, regressions performed at the low-frequency level, at this level the

//db.nomics.world/OECD/EO?q=OECD%2FEO%2FOTO.CPI_YTYPCT.Q) and the nominal interest rates (https://db.nomics.world/OECD/EO?dimensions=%7B%22VARIABLE%22%3A%5B%22IRS%22%5D%7D&q=OECD%20economic%20outlook%20interest%20rate) are obtained from the *OECD Economic Outlook* database. The aggregate interest rate is the weighted average of the rates in the OECD countries. Annual CO_2 emissions, which correspond to the emissions from the burning of fossil fuels for energy and cement production, are from *Our World In Data* (https://ourworldindata.org/explorers/co2?facet=none&country=~OWID_WRL&Gas+or+Warming=CO2&Accounting=Territorial&Fuel+or+Land+Use+Change=All+fossil+emissions&Count=Per+country). We convert annual data into quarterly data using the same disaggregation approach as for GDP. Our solution method explicitly deals with trends and thus does not impose that variables must return to the steady state. [15] Consequently, we simply use the growth rate (i.e., the first difference of the logarithm) for GDP and CO_2 emissions and maintain the level of inflation and interest rates. Figure 1 displays the temporal evolution of all the observable variables of the model. The measurement equations mapping our model to the four observable macroeconomic and climate-related time series are given by:

$$\begin{bmatrix} \text{Real output growth rate} \\ \text{Inflation rate} \\ \text{Short-term interest rate} \\ \text{CO}_2 \text{ emissions growth rate} \end{bmatrix} = \begin{bmatrix} \Delta \log (y_t) \\ \pi_t - 1 \\ r_t - 1 \\ \Delta \log (e_t) \end{bmatrix}. \tag{22}$$

FIGURE 1. Observable variables

target time series and the indicator time series are both available. Second, the resulting estimates are used to obtain the high-frequency target series.

[15] Linearization methods impose to approximate any model's decision rules around a fixed point, and therefore, impose that the model is stationary in the neighborhood of the fixed point. Thus, the inference must be assessed based on stationary data, the latter implies a set of transformations (e.g., dividing by population, business cycle filters, etc.).

3.3. **Calibrated parameters.** A first set of parameters is calibrated. These parameters can be divided into two groups: the structural parameters and initial conditions. We begin by discussing the calibration of the structural parameters reported in Panels A and B of Table 1.

TABLE 1. Calibrated parameter values and initial conditions (quarterly basis)

NAME	PARAMETER	VALUE
Panel A: Climate Parameters		
Marginal atmospheric retention ratio	ξ_m	0.27273
Pre-industrial stock of carbon (GtC)	m_{1750}	545
Climate damage elasticity	γ	3.569e-05
Abatement cost curvature	θ_2	2.6
Decay abatement cost	δ_{pb}	0.004277
Panel B: Economic Parameters		
Firm exit shock	ν	0.05
Low productivity worker payoff-to-consumption	d/c	0.97
Share low productive workers	ω	0.02
Terminal population (billion)	l_∞	10.48
Population growth	l_g	0.00625
Goods substitution elasticity	ς	4
Decay TFP (annualized)	δ_z	0.0018
Decay rate emission intensity	δ_σ	0
Labor intensity	α	0.7
Long-term inflation target	$\pi^\star_\infty$	0.0025
Discount factor	β	0.99733
Panel C: Initial Conditions		
Initial GDP (trillion USD PPP)	y_{t_0}	7.5
Initial inflation trend (annualized)	$\pi^\star_{t_0} \times 400$	10
Initial emissions ($GtCO_2$)	e_{t_0}	5.075
Initial abatement cost-to-gdp	θ_{1,t_0}	0.31907
Initial population (billion)	l_{t_0}	4.85
Initial stock of carbon (GtC)	m_{t_0}	719.94
Initial carbon price ($/ton)	τ_{e,t_0}	0
Initial hours worked	h_{t_0}	1
Initial interest rate	r_{t_0}	5/400

These parameters are categorized into three panels. Panel A is related to the climate dynamics. Parameter ξ_m simply converts CO_2 units into carbon units as follows: GtC = ξ_m $GtCO_2$ (as damages are typically measured by the radiative forcing from carbon), while m_{1750} is the natural stock of carbon in the atmosphere back in 1750. The last parameter, γ, maps carbon stock to economic damage. Because temperatures and carbon stock are cointegrated variables, we follow Golosov et al. (2014) and assume that damage directly emerges from atmospheric carbon concentration. Parameter γ is set to 5.57e-5 to entail a permanent 5%

output loss in the business-as-usual scenario in a similar fashion as in Barrage and Nordhaus (2024). Note that this parameterization is higher than that in Golosov et al. (2014) to match the increased damage, by a factor of two, in DICE 2023 compared to its 2016R2 counterpart. Regarding the abatement sector, we build on Barrage and Nordhaus (2024). The curvature of abatement cost function θ_2 is strongly convex and fixed at 2.6.

Panel B shows the calibration of the economic parameters. The discount factor is set to match the average real interest rate in the sample. Regarding the discounting of the Euler and Phillips curves, the exit rate ν is taken from the firm entry literature and assumes a 5% rate, consistent with OECD data documenting the death rates in the manufacturing and services sectors. In contrast, the Euler discount depends on ω and d; we impose a calibration such that we obtain a 3% percent discount as in McKay et al. (2017) by imposing a fraction of 2% of workers experiencing the income shock, while the insurance is set to 95% of consumption. Regarding the calibration for the exogenous process for the population, the population at the start of the sample (1984Q4) is set at 4.85 billion, but will converge at an annual 2.5% rate toward the long-term population $l_\infty = 10.48$ billion, consistent with United Nations forecasts for 2100. The substitutability of intermediate goods provides a 33% markup, which is typical of calibrating macroeconomic models with imperfect competition. The growth decay parameters δ_z and δ_σ are obtained from DICE 2023.

Panel C reports the initial conditions required to pin down all the state variables of the model prior to its estimation at t_0 in 1984Q4. The labor supply is normalized to one, while the labor intensity is set to 0.7, as in DICE. Finally, regarding the exogenous process for the inflation target, we minimize the difference with the inflation data, and obtain an initial inflation target of 10% annually, with a decay rate of 7.5% per year to reach a long-term inflation target of 1%. Finally, to capture realistic levels of GDP and CO_2 emissions, we set the level of GDP to 7.5 trillions USD and the level of emissions to 5 $GtCO_2$, as in 1984. The initial population, GDP, interest rate, and emissions are set to their observable values in 1984Q4. Based on atmospheric carbon concentrations, we estimate the initial carbon stock m_{t_0} to be 719 GtC in 1984Q4. From this, we compute the corresponding damages and determine the initial level of hours worked to calibrate the disutility of labor, ψ. Using the production function and given y_{t_0}, we derive the initial total factor productivity (TFP), z_{t_0}. Regarding the level of the abatement cost function θ_{1,t_0}, following Barrage and Nordhaus (2024), it is calibrated to reach 10.9% of GDP in 2020 under full abatement ($\mu = 1$). Since our first simulation date is much

earlier, we extrapolate this value back to $t_0 = 1984Q4$, resulting in an estimated value of approximately 31.9%. Technological progress in δ_{pb}, driven by the adoption of cost-efficient technologies, reduces the abatement cost by 1.7% per year, consistent with the DICE model. For the initial carbon stock in our simulation, we set its 1984 value to 719 GtC, based on historical carbon concentration data.

The last variable that requires discussion is the expected path of the carbon tax $\tilde{\tau}_{e,t}$. The transition scenario occurring out-of-sample influences expectations, thereby altering the data representation provided by the estimated model. Rather than imposing an arbitrary mitigation scenario (such as the Paris Agreement), we let the data inform the expected path of the carbon tax. Let $\{\tilde{\tau}^{\star}_{e,t}\}^{T}_{1984Q4}$ represent the carbon tax trajectory under temperature stabilization by 2050, consistent with the Paris Agreement. [16] Since agents may not fully believe in the realization of this scenario, we allow for the following expectation scheme: $\mathbb{E}_{t,t+S}\{\tilde{\tau}_{e,t}\} = \varphi\tilde{\tau}^{\star}_{e,t}$, where $\varphi \in [0,1]$ represents the market belief in the realization of the Paris Agreement. The parameter φ can be interpreted as *(i)* the prior probability of the mitigation policy's realization, *(ii)* the fraction of agents who believe in a complete mitigation policy, or *(iii)* the belief in the policy's stringency.

3.4. **Prior and posterior distributions.** The remaining parameters are estimated. Their prior distributions are presented in Table 2.

The exogenous shocks are distributed according to an inverse gamma "type 2" as in Christiano et al. (2014), with a prior mean of 0.002 and a standard error of 0.0033. The AR coefficients of the shock processes follow a Beta distribution with a prior mean of 0.5 and a standard deviation of 0.1, which is a relatively more informative prior than in Smets and Wouters (2007). Regarding structural parameters, we estimate the annualized slope of TFP growth and carbon decoupling. In DICE models, these parameters typically lie between 1% and 1.5%. Therefore, we impose a diffuse Gamma distribution with a mean of 1.5 and a standard deviation of 0.5. The prior of the utility parameter determining labor supply σ_l is taken from Smets and Wouters (2007) with a Gamma distribution to impose a positive support for its posterior distribution. The risk aversion σ_c is given a prior mean of 2.5 to match the relatively higher risk aversion parameter in emerging market economies (e.g., Aguiar and Gopinath

[16] Formally, it is assumed that the Paris Agreement-consistent tax path increases linearly from 2023Q3 to 2050Q1, starting at 0 $ per ton of carbon and reaching 152 $ to align with the backstop price of carbon under a full mitigation policy. Beyond this period, the carbon price naturally declines due to the decreasing cost of abatement, consistent with DICE.

2007), thus attenuating the transmission channel of monetary policy. The Rotemberg adjustment cost parameter κ is typically between 20 and 200 in the literature. Accordingly, we impose a Gamma distribution with a prior mean of 30 and a standard deviation of 10. Next, we discuss the parameters related to monetary policy. For the reaction coefficient on inflation, we consider the prior distributions of Smets and Wouters (2007), and take a Gamma shape for $\phi_\pi - 1$ to ensure that the Taylor principle holds for any posterior value. ϕ_y follows the prior of Smets and Wouters (2007) but with a Gamma distribution. Finally, the mitigation belief probability φ follows a Beta distribution with a prior mean of 0.5 and a standard deviation of 0.1.

TABLE 2. Prior and posterior distributions of structural parameters

		Prior Distribution			Posterior Distribution		
		Shape	Mean	Std	Mode	Mean	[5%:95%]
Panel A: Shock processes							
Std demand	σ_b	$\mathcal{IG}_2$	0.002	0.0033	0.0297	0.0284	*[0.0250:0.0319]*
Std price	σ_p	$\mathcal{IG}_2$	0.002	0.0033	0.0204	0.0206	*[0.0182:0.0230]*
Std MPR	σ_r	$\mathcal{IG}_2$	0.002	0.0033	0.0009	0.0009	*[0.0008:0.0010]*
Std emissions	σ_e	$\mathcal{IG}_2$	0.002	0.0033	0.0050	0.0050	*[0.0045:0.0056]*
AR demand	ρ_b	$\mathcal{B}$	0.5	0.1	0.7714	0.7578	*[0.7234:0.7829]*
AR price	ρ_b	$\mathcal{B}$	0.5	0.1	0.9767	0.9686	*[0.9562:0.9788]*
AR MPR	ρ_r	$\mathcal{B}$	0.5	0.1	0.7631	0.7033	*[0.5987:0.7918]*
AR emissions	ρ_e	$\mathcal{B}$	0.5	0.1	0.9615	0.9638	*[0.9533:0.9747]*
Panel B: Structural parameters							
Initial TFP growth	$g_{z,t_0} \times 400$	$\mathcal{G}$	1.5	0.5	1.9598	1.9672	*[1.9348:2.0053]*
Decay rate decoupling	g_{σ,t_0}	$\mathcal{G}$	1.5	0.5	1.3519	1.3225	*[1.2677:1.3918]*
Risk aversion	σ_c	$\mathcal{G}$	2.5	0.2	1.9440	1.8941	*[1.6856:2.1008]*
Labor disutility	σ_h	$\mathcal{G}$	2	0.75	0.2483	0.3469	*[0.2002:0.5312]*
Rotemberg Cost	κ	$\mathcal{G}$	30	10	187.33	187.33	*[187.32:187.33]*
Decline rate inflation target	$\rho_{\pi^\star}$	$\mathcal{N}$	0.02	0.005	0.0188	0.0196	*[0.0140:0.0246]*
Initial interest rate	$r_{t_0} \times 400$	$\mathcal{N}$	12	2	8.7767	8.4984	*[7.9540:9.0021]*
Inflation stance	$(\phi_\pi - 1)$	$\mathcal{G}$	0.75	0.1	0.5042	0.5068	*[0.3813:0.6258]*
MPR GDP stance	ϕ_y	$\mathcal{G}$	0.12	0.05	0.0798	0.0844	*[0.0519:0.1257]*
Discount rate	$(\beta^{-1} - 1) \times 100$	$\mathcal{G}$	0.8	0.2	0.2676	0.2839	*[0.1950:0.3758]*
Mitigation policy belief	φ	$\mathcal{B}$	0.5	0.15	0.4877	0.5695	*[0.3802:0.7442]*
MPR smoothing	ρ	$\mathcal{B}$	0.5	0.1	0.7763	0.7894	*[0.7255:0.8455]*
Log marginal data density							-2967.97

Note: $\mathcal{B}$ denotes the Beta, $\mathcal{G}$ the Gamma, $\mathcal{N}$ the Gaussian, and $\mathcal{IG}_2$ the Inverse Gamma (type 2) distributions. A total of 120,000 draws were used to compute the posterior mean and 90% confidence interval.

We next turn to the posterior distribution generated by the Metropolis-Hasting sampler, expressed in 90% confidence intervals in Table 2. The price mark-up shock has the largest persistence, as is also found by Smets and Wouters (2007). In addition, the pollution shock also exhibits significant persistence, as obtained by Jondeau et al. (2023). The initial productivity growth is, on average, above the values found in DICE, but this is not surprising as our

initial period of simulation (1985) exhibits higher TFP Growth than the 2015-2020 period of DICE. Similar patterns are also observed for the decoupling rate. In comparison to Smets and Wouters (2007), we observe a much flatter labor supply equation, which causes the marginal cost and thus the inflation rate to be less responsive to a change in hours. Rotemberg price stickiness parameter takes on a large value, suggesting a very flat Phillips curve consistent with a lot of evidence covering the Great Moderation period. The smoothing of the interest rate is similar to that reported by Smets and Wouters (2007), whereas the reaction coefficient on inflation is relatively smaller. Finally, the model's estimation suggests that agents attached a probability of approximately 56% to achieving the goals under the Paris agreement.

Appendix C provides an assessment of the model's fit. It compares the empirical and model-implied moments. It shows the generalized impulse response functions of the four shocks, as well as the historical decomposition of detrended output, inflation and the nominal interest rate. Overall, the estimated model does a reasonable job in accounting for the empirical features of the four observables.

4. The anatomy of the green transition

In this section, we analyze how climateflation and greenflation phenomena may affect the world economy by 2100. The first stage of this analysis relies on long-term projections derived from the model under alternative scenarios. We then, decompose output and inflation into macroeconomic and environmental drivers.

4.1. **Model-implied projections under CO2 emission scenarios.**

We begin by presenting long-term projections from the model to illustrate what would happen for the global economy by 2100. To this end, three alternative scenarios are implemented in Figure 2, differing only in the degree of effective implementation, summarized by φ. [17] The first scenario in green aligns with the SSP1-1.9 pathway from IPCC (2021), representing carbon emissions consistent with the effective realization of the Paris Agreement ($\varphi = 1$). The second scenario in red corresponds to the SSP3-7.0 pathway from IPCC (2021), where agents receive news of no carbon tax implementation ($\varphi = 0$), leading to a continuous increase in carbon emissions (*laissez-faire*). The third scenario in blue lies between these extremes and assumes a carbon tax process (*estimated tax path*) that reflects household expectations. The future path of the carbon

[17] In 2023Q3, all agents receive information about a shift in carbon tax policy intensity, which could correspond to the laissez-faire scenario with $\varphi = 0$ or the Paris Agreement scenario with $\varphi = 1$.

FIGURE 2. Model-implied projections based on alternative control rates of emissions

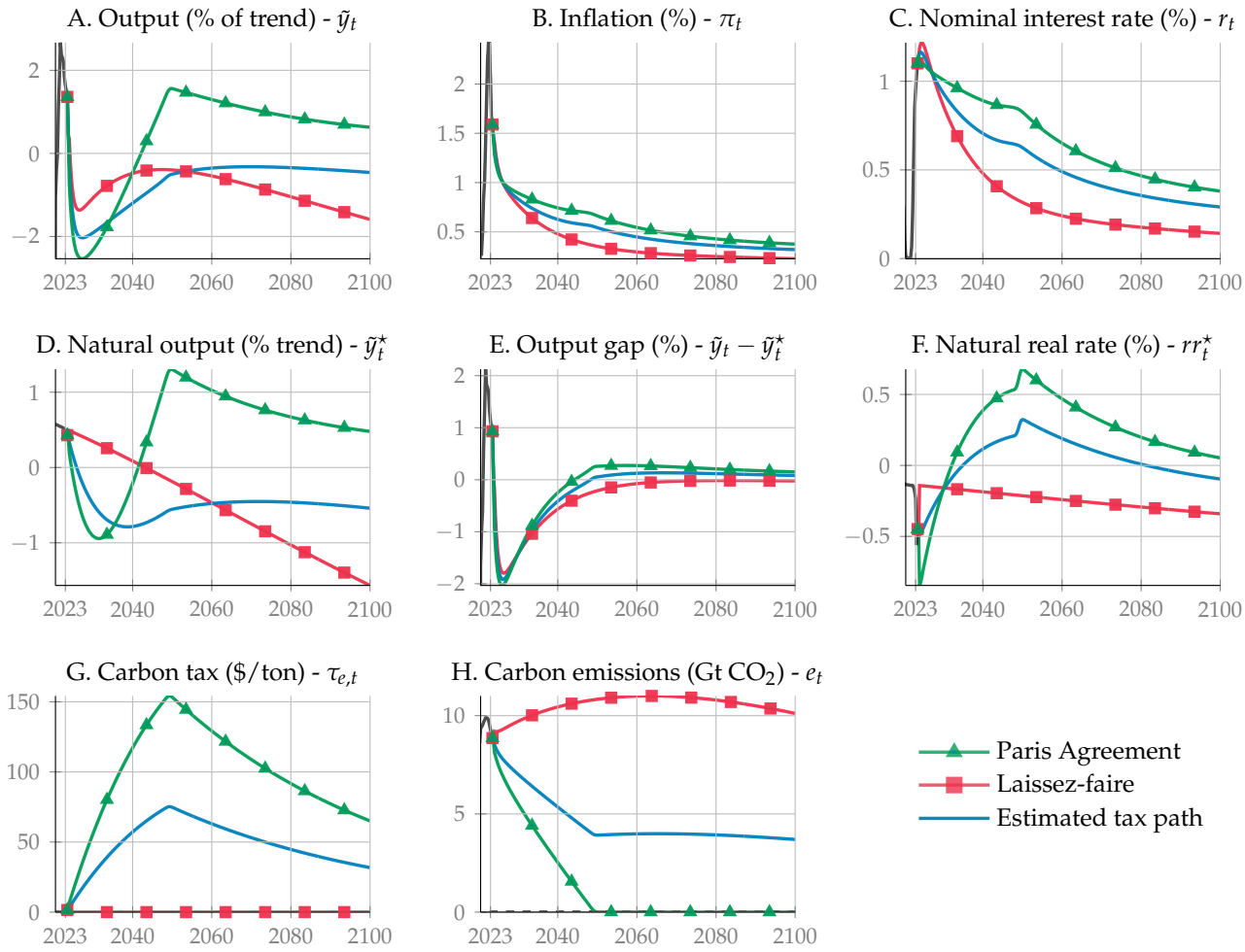

Note: This figure displays the projections of the main variables of the New-Keynesian climate model under three scenarios: *(i)* the Paris Agreement (carbon tax consistent with net zero in 2050), *(ii)* laissez faire (no carbon tax), and *(iii)* carbon tax consistent with the forecasts of the estimated model.

tax rate is announced in 2023Q3, with expectations adjusting immediately in response to the new environment. [18] Importantly, this analysis focuses on climate change mitigation rather than the optimal tax design, which is specifically addressed in the robustness section.

In the laissez-faire scenario, where no emission control measures are implemented and the carbon tax remains zero, climate damages steadily increase over time. This leads to a gradual decline in total factor productivity (TFP), natural output, and the natural real interest rate (Panels D and F). In 2023, the economy begins to recover from the energy price shock

[18] Note that all forecasts are driven by four main forces, which differ significantly from the typical shock analysis in New Keynesian models. These forces are: (i) the exogenous processes based on their in-sample realizations, (ii) the deterministic trend processes gradually converging toward their terminal states, (iii) the carbon price policy effectively implemented, and (iv) the accumulation of atmospheric carbon, which causes permanent damage to the economy.

recession, but output rapidly falls below the technological neutral trend due to accumulating climate damages, causing GDP to drop close to 2% below trend. The anticipated decline in demand (Panel A) further drives inflation downward (Panel B), falling below the baseline blue scenario. [19] In response to these negative developments, the central bank lowers its policy rate (Panel C).

The economy evolves quite differently under the Paris Agreement scenario. In this scenario, a carbon tax is implemented, which gradually increases and eventually reaches a level of $150 per ton of emissions in 2050. This is the carbon tax that is needed to achieve the transition to a net-zero carbon economy (Panels G and H). In this case natural output initially falls due to the rise in taxes and the increase in abatement costs, but subsequently rises as abatement expenditures boost aggregate demand. A qualitatively similar pattern is followed by the natural real interest rate (Panel F). One notable consequence of the investment-led expansion is the emergence of more persistent inflationary pressure. While the output gap gradually closes under laissez-faire, it overshoots under the Paris agreement (Panel E). The joint combination of the rising carbon taxes and increased demand due abatement expenditures contributes to a surge in inflation, which we term "greenflation." As a result monetary policy needs to tighten as shown in Panel C.

Given the simplicity of our model, we leverage its tractability to conduct a straightforward decomposition analysis of aggregate demand and supply schedules during the transition, enabling us to examine the various forces driving output and inflation.

4.2. **Decomposing output.** In this section we examine the various forces that influence total output. From the resource constraint, the logarithm of the detrended output ($\hat{y}_t = \log(\tilde{y}_t/\tilde{y})$) can be approximated as follows: [20]

$$\hat{y}_t \simeq \underbrace{\widehat{IS}_t}_{\text{consumption}} + \underbrace{\theta_{1,t}\tilde{\tau}_{e,t}^{\theta_2/(\theta_2-1)}}_{\text{abatement expenditures}} + \underbrace{(1-\vartheta)\frac{\kappa}{2}(\pi_t-\pi_t^\star)^2+\vartheta(1-mc_t)}_{\text{nominal costs}}. \tag{23}$$

Three main forces can be distinguished. The term $\widehat{IS}_t$ captures the standard permanent income and intertemporal substitution effect on **consumption**. [21] This term also captures the

[19] Climate damages resemble a persistent supply shock, a dynamic extensively analyzed in Nuño et al. (2024) for monetary policy implications.

[20] See Appendix D for details on obtaining this approximation.

[21] $\widehat{IS}_t = \log(IS_t/IS)$ where $IS_t = \omega\tilde{d}_t + (1-\omega)\left[\omega\mathbb{E}_t\left\{\sum_{s=0}^{\infty}\beta(1-\omega)^s\varepsilon_{b,t+s}\tilde{d}_{t+s}^{-\sigma_c}\prod_{j=0}^{s}\frac{r_{t+j}}{\pi_{t+1+j}}\right\}\right]^{-1/\sigma_c}$.

main channel of monetary policy transmission, which compared to the standard New Keynesian model is attenuated by the assumed discounting in the Euler equation. The second term, **abatement expenditures**, captures the autonomous spending on abatement that is necessary to reach net zero emissions in 2050. The last term, named **nominal costs**, captures the menu costs of inflation and the consumption of dividends for firms exiting the market.

FIGURE 3. Decomposition of detrended output during the transition

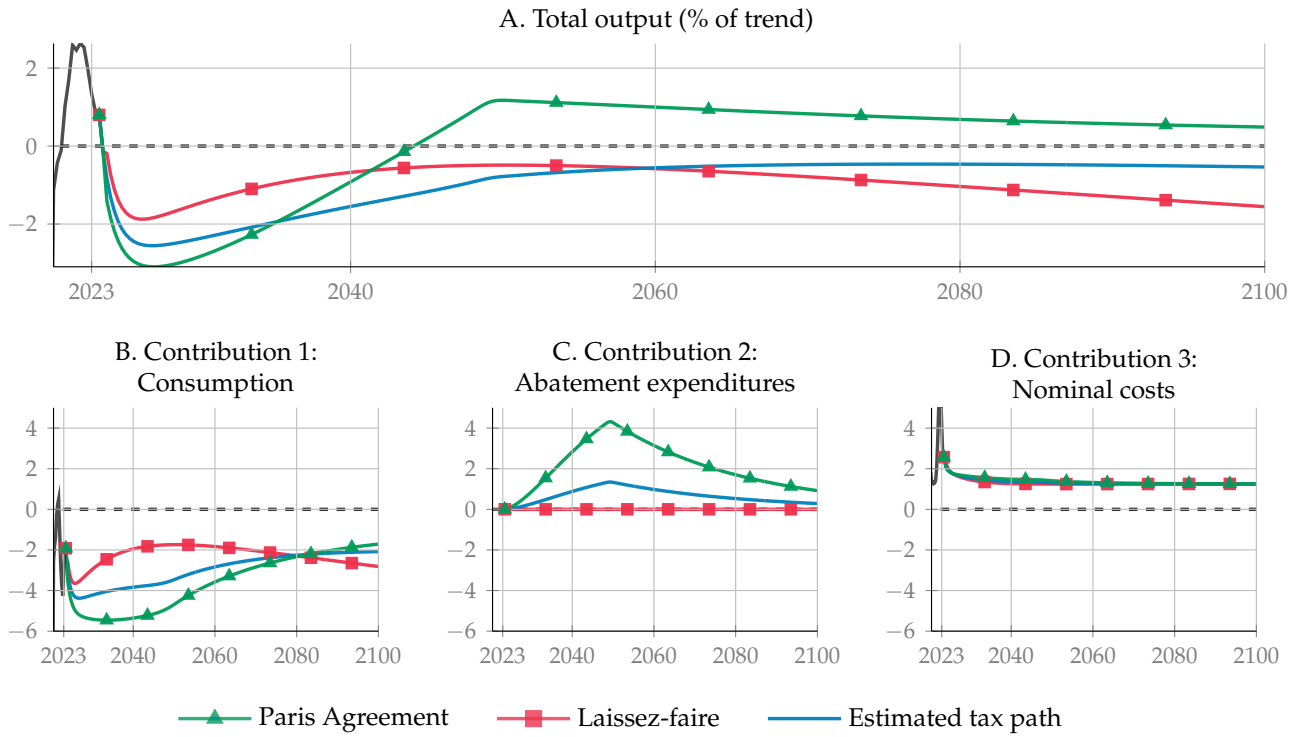

Note: This figure displays the projections of the detrended output under three scenarios: *(i)* the Paris Agreement (carbon tax consistent with net zero in 2050), *(ii)* laissez faire (no carbon tax), and *(iii)* carbon tax consistent with the forecasts of the estimated model.

Figure 3 presents the decomposition of detrended output into three components across the three scenarios (note that Panel A is the sum of Panels B, C, and D). It is insightful to compare the Paris Agreement scenario (green line) and the laissez-faire scenario (red line) with the baseline scenario under the estimated carbon tax path (blue line). In the Paris Agreement scenario, the rise in carbon taxes initially leads to a deeper recession compared to the baseline, which subsequently transitions into a boom as abatement spending increases to over 4% at the peak of the transition. This relatively deeper initial recession is driven by the negative supply effects of higher taxes and their crowding out of consumption (Panel B). Monetary policy responds by tightening due to the inflationary pressures from higher

tax-induced costs. Interestingly, the inflation costs (Panel D) are similar across all transition types, primarily reflecting the initial cost-push shock from the Ukraine war.

In contrast, the laissez-faire scenario begins with a shallower initial recession (relative to the baseline) as the absence of current and expected carbon taxes temporarily boosts output. However, as economic damages to productivity from a warming planet accumulate, output eventually falls below the baseline level. This anticipated decline in future output is mirrored in reduced consumption, which contributes to comparatively lower inflationary pressures. Climate change thus transmits to output through the IS equation, as intertemporal substitution leads agents to feel poorer, prompting increased savings to smooth consumption over time.

4.3. **Decomposing inflation.** We proceed in the same way to analyze the various forces that influence inflation. The Phillips curve is a highly nonlinear equation. In order to keep track of most nonlinearities in the decomposition, we propose a semi-linearization approach, which allows us to decompose the "inflation gap" ($\hat{\pi}_t = \pi_t - \pi_t^\star$) into four drivers:

$$\hat{\pi}_t \simeq \underbrace{\hat{\pi}_t^w}_{\text{real wage}} + \underbrace{\hat{\pi}_t^c}_{\text{climateflation}} + \underbrace{\hat{\pi}_t^g}_{\text{greenflation}} + \underbrace{\hat{\pi}_t^x}_{\text{exogenous shocks}}, \tag{24}$$

with

$$\hat{\pi}_t^j = \frac{\xi - 1}{\kappa} \widehat{mc}_t^j + \mathbb{E}_t\{\beta_{t+1}^\pi \hat{\pi}_{t+1}^j\} \quad \text{for } j = \{w, c, g\},$$
$$\hat{\pi}_t^x = \frac{\xi - 1}{\kappa} \left(\varepsilon_{p,t} - 1\right) mc_t + \mathbb{E}_t\{\beta_{t+1}^\pi \hat{\pi}_{t+1}^x\},$$

where $\beta_{t+1}^\pi = (1 + g_{z,t+1})\, \tilde{y}_{t+1}/\tilde{y}_t$ is the discount factor adjusted by GDP growth, and $\widehat{mc}_t^j$ are the elements obtained from the linear approximation of the marginal cost expression: [22]

$$mc_t = \underbrace{\frac{\psi \left(x_t \tilde{y}_t - \omega \tilde{d}_t\right)^{\sigma_c} \tilde{y}_t^{\frac{1+\sigma_n}{\alpha} - 1}}{(1-\omega)^{\sigma_c + \sigma_n}}}_{mc_t^w} \underbrace{\frac{1}{\Phi \left(\tilde{m}_t\right)^{\frac{1+\sigma_n}{\alpha}}}}_{mc_t^c} + \underbrace{\tilde{\tau}_{e,t} \theta_{1,t} \left(\theta_2 + \tilde{\tau}_{e,t}^{\frac{1}{\theta_2 - 1}} (1 - \theta_2)\right)}_{mc_t^g} \tag{25}$$

The term mc_t^w represents the standard component of marginal cost, influenced by real wages through the general equilibrium mechanism. The term mc_t^c arises from the damage function, which reduces total factor productivity (TFP) and increases marginal costs as carbon emissions intensify. This term is relatively exogenous, as it responds only modestly to

[22] See Appendix D for details on obtaining this approximation.

general equilibrium variables such as output and inflation, with its rate of growth adjusting proportionally to the carbon tax. Finally, the term mc_t^g is associated with the implementation of a carbon tax and the related abatement expenses, which further increase the firm's marginal cost. This term is purely exogenous, as it depends solely on the effective realization of the carbon tax.

FIGURE 4. Decomposition of inflation during the green transition

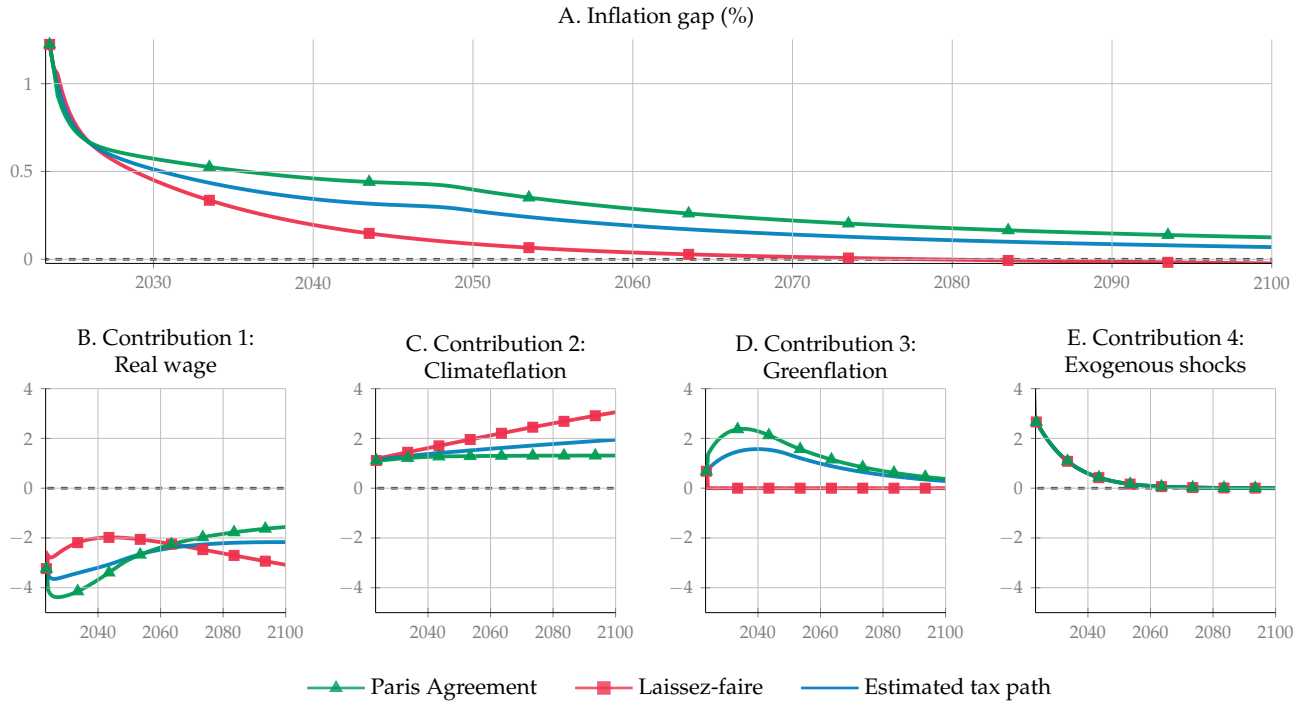

Note: This figure displays the projections of the inflation gap (inflation relative to its target) under three scenarios: *(i)* the Paris Agreement (carbon tax consistent with net zero in 2050), *(ii)* laissez faire (no carbon tax), and *(iii)* carbon tax consistent with the forecasts of the estimated model.

Figure 4 illustrates the contribution of each component to inflation under the three alternative scenarios. The dynamics of the inflation gap are broadly similar across scenarios, partially driven by a disinflation process as the estimated positive cost-push shocks dissipate toward the end of the sample (Panel E). However, as previously discussed, inflation is significantly more persistent under the Paris Agreement scenario. By 2050, inflation is 0.3 percentage points (1.2 percentage points annualized) higher than in the laissez-faire scenario. This quantitative measure of greenflation is remarkably in line with large-scale model of Coenen et al. (2024), but much higher than Olovsson and Vestin (2023). The decomposition reveals that under the Paris Agreement, the contribution of climateflation caused by global warming is lower than in the baseline scenario, stabilizing at 0.6 percentage points toward the end

of the century (Panel C). However, the higher carbon taxes and related abatement expenditure costs result in a greater contribution from greenflation, which peaks at over 2 percentage points in 2030. A strong general equilibrium effect from wage-setting mechanisms attenuates inflationary pressures from both climateflation and greenflation. Specifically, the crowding-out effect of abatement expenditures on consumption shifts the wealth effect in labor supply, inducing a strong decline in real wages. Overall, the adjustment in real wages fails to offset the inflationary pressures, resulting in a more inflationary environment.

In contrast, under the laissez-faire scenario, the contribution of climateflation, $\hat{\pi}_t^c$, steadily rises above that in the baseline, exceeding 3 percentage points by the end of the century as damages to productivity continuously increase due to global warming. However, this inflationary effect of climate change is more than offset by the negligible contribution (zero) of greenflation. Additionally, while real wages initially decline less in this scenario, they become increasingly affected by the ongoing reduction in productivity caused by global warming. [23] Indeed, we find that the general equilibrium effects from wage adjustments are sufficient to attenuate climateflation. In the robustness section of the paper, we examine how this mechanism changes under conditions of wage stickiness.

In summary, our framework reveals that stronger mitigation policies are more inflationary, as the greater impact of greenflation outweighs the reduction in climateflation. This dynamic is closely tied to the ability of wage adjustments to mitigate the forces of both climateflation and greenflation.

In Appendix E, we conduct a sensitivity analysis to examine the effects of various structural parameters on inflation, output and interest rate dynamics during the green transition. We investigate the effects of changes in the degree of discounting, the monetary policy reaction coefficients, the slopes of the aggregate demand and Phillips curves and climate-related parameters. In brief, we find that the inflationary effects of the green transition are larger: (i) the less forward-looking households are; (ii) the more forward-looking price setters are; (iii) the weaker (stronger) the central bank reacts to inflation (the output gap); (iv) the steeper the slope of the Phillips curve; and (v) the lower the interest elasticity of consumption. Not surprisingly, the inflationary effects of the green transition also rise with higher abatement costs.

[23] Our decomposition exercise is based on a nonlinear model, where cross-products are not eliminated through linearization. As a result, the factors are not orthogonal, i.e., $cov\left(\hat{\pi}_t^g, \hat{\pi}_t^w\right) \neq 0$.

Instead, a rise in the damages from global warming has less of an impact on the inflationary consequences of the green transition.

5. Climate change and monetary policy

This section examines the relationship between climate change and monetary policy, as extensively discussed by Schnabel (2022). Specifically, it highlights how the central bank's inflation/output trade-off is affected by the structural change associated with climate change and mitigation policies and how the design of the monetary policy rule influences the impact of climate change on the broader economy.

5.1. **Managing the inflation/output tradeoffs in the presence of climate change.** Figure 5 shows the impact of climate change and mitigation policies on the central bank's tradeoff between inflation and output stabilisation. The inflation-output variability frontier is plotted over two horizons and for the two transition scenarios (*Paris Agreement* and *laissez faire*). The two horizons correspond to the medium run, i.e. the transition period from 2024 to 2050, and to the long run, i.e. after the transition from 2050 to 2100.

FIGURE 5. Inflation-output variability frontier under alternative output gap weight in the Taylor rule

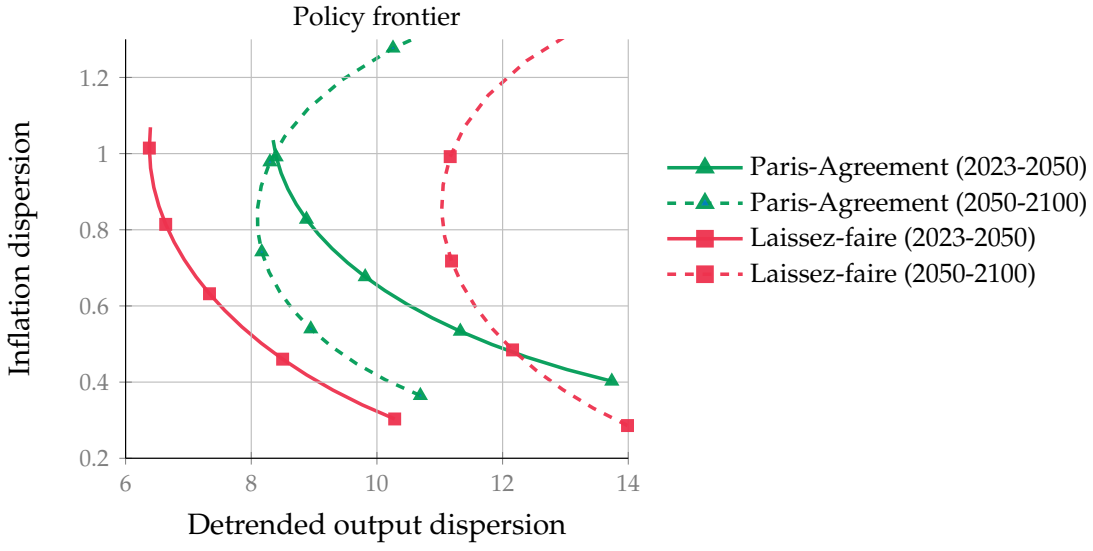

Note: This figure illustrates the dispersion of inflation (y-axis) and detrended output (x-axis) for different values of the parameter ϕ_y under two scenarios: *(i)* the Paris Agreement (green) and *(ii)* laissez-faire (red). Inflation dispersion is defined as $\mathbb{E}\{(\pi_t - \pi_t^\star)^2\}$, and output dispersion is defined as $\mathbb{E}\{(\tilde{y}_t - \tilde{y})^2\}$. These dispersions are calculated by sampling shocks across 50 independent chains, with each dispersion representing the average squared deviation over a specified period (e.g., 2023Q1–2050Q2) and all 50 draws.

The figure illustrates how during the transition period the Paris Agreement shifts the inflation/output variability frontier to the right relative to the laissez-faire scenario. Depending on its loss function, the central bank can limit the rise in inflation volatility by allowing larger output volatility or the reverse. But it can not avoid that the mitigation of climate change worsens the trade-off in the transition period. This aligns well with the findings of Del Negro et al. (2023), who identify similar dynamics in a multi-sector framework, and resonates with the insights of Schnabel (2022) highlighting the supply-side nature of the greenflation shock.

The medium-term stabilisation costs of mitigation are, however, compensated by a much more favourable trade-off in the long run. Indeed, in the long run inflation/output variability frontier shifts inward facilitating the stabilisation of the economy. The mitigation policies under the Paris Agreement, while costly in the medium term, lay the groundwork for a more stable economic environment post transition. By contrast, under laissez-faire the absence of climate-mitigation efforts results in relatively lower inflation and output variability in the medium run, but generates much higher economic dispersion in the future.

In summary, this exercise highlights the short-term cost of increased inflation due to greenflation and the long-term benefits of reduced GDP dispersion over time.

5.2. **Natural rates and the design of the monetary policy rule.** As discussed in subsection 4.1, climate change and associated mitigation policies have a profound medium-term impact on the level and growth rate of natural output and the natural real interest rate. As highlighted by Orphanides (2002), the misperception of these natural rates in the monetary policy rule can have detrimental implications for the effective stabilisation of inflation. In this section, we investigate the impact of alternative assumptions about natural output and the natural interest rate in the monetary policy rule for the evolution of the economy under the Paris Agreement scenario.

For that, we express the monetary policy rule as a generic function of the couple $(\varsigma_{r,t}, \varsigma_{y,t})$ as follows:

$$\varsigma_{r,t} = \varsigma_{r,t-1}^{\rho} \left[\frac{\pi_t^\star}{\pi} \left(\frac{\pi_t}{\pi_t^\star} \right)^{\phi_\pi} \varsigma_{y,t}^{\phi_y} \right]^{1-\rho} \varepsilon_{r,t}. \tag{26}$$

We consider three cases. The estimated baseline rule, denominated R_b, is the most widespread rule in macroeconomic models (e.g. Smets and Wouters, 2007). It is given by:

$$(\varsigma_{r,t}, \varsigma_{y,t}) = \left(\frac{r_t}{r}, \frac{\tilde{y}_t}{\tilde{y}_t^\star} \right). \tag{27}$$

In this rule, the nominal interest rate is expressed as a deviation from its constant long-term level, while output is measured relative to its time-varying natural level, which accounts for the effects of climate change. However, any quantitative outcome based on this rule, such as in Smets and Wouters (2007), may risk targeting a return to a steady-state interest rate, even when the economy has undergone a permanent shift due to climate impacts or mitigation policies.

However, as discussed before, the determinants that affect the natural output level also affect the natural interest rate (Laubach and Williams, 2003, Holston et al., 2017). Consequently, using a steady-state interest rate as a reference to set the current policy rate may be misleading. An alternative approach is to express also the interest rate in deviations from its natural rate. This rule, denominated $R_\star$, is given by:

$$(\varsigma_{r,t}, \varsigma_{y,t}) = \left(\frac{r_t}{r_t^\star \pi_t^\star}, \frac{\tilde{y}_t}{\tilde{y}_t^\star} \right). \tag{28}$$

The third case is closer to the classical Taylor rule, which assumes not only a constant equilibrium real interest rate, but also a deterministic path for the real economy that does not take into account the impact of damages coming from climate change. This rule, denominated R_{ss}, is given by:

$$(\varsigma_{r,t}, \varsigma_{y,t}) = \left(\frac{r_t}{r}, \frac{\tilde{y}_t}{\tilde{y}} \right). \tag{29}$$

Figure 6 reports the path of the economy under the three different types of monetary policy rules. Among these three rules, the most efficient rule for stabilizing inflation is the one that takes into account both the natural level of output and the natural real interest rate. Under both climate change scenarios inflation converges more quickly towards the inflation target of 1%. The cost in terms of a larger deviation of output from its steady state level is limited. By anchoring policies to the natural rates, a central bank can better stabilize the economy.

In contrast, if the central bank ignores the effects of climate change and the mitigation policies on the natural output and real interest rate in its policy rule, inflation remains persistently above target till the end of the century. This is most striking in the Paris Agreement scenario. However, it also shows up in the laissez-faire scenario. In that case, ignoring the increasing damages from global warming on productivity results in a rise in inflation in the second half of this century.

FIGURE 6. The impact of climate transition under alternative monetary policy rules

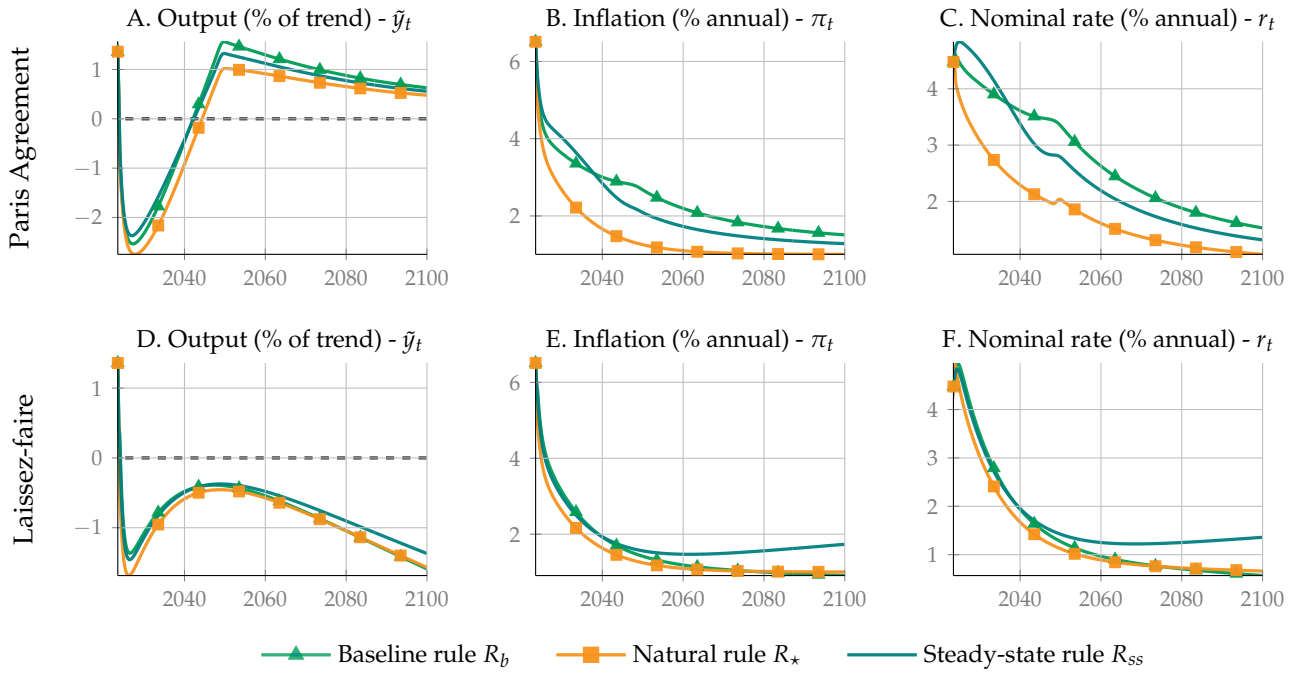

Note: This figure displays the paths of the key variables consistent with the Paris Agreement scenario under *(i)* the estimated policy rule where $(\varsigma_{r,t}, \varsigma_{y,t}) = (r_t/r, \tilde{y}_t/\tilde{y}_t^\star)$ (green line), *(ii)* a policy rule adjusted with the natural real rate where $(\varsigma_{r,t}, \varsigma_{y,t}) = (r_t/(r_t^\star \pi_t^\star), \tilde{y}_t/\tilde{y}_t^\star)$ (orange line), and *(iii)* a policy rule in which the variables deviate from their steady-state levels where $(\varsigma_{r,t}, \varsigma_{y,t}) = (r_t/r, \tilde{y}_t/\tilde{y})$ (blue line).

6. THE SOCIAL COST OF CARBON

This section examines the concept of the social cost of carbon (SCC) within our New Keynesian framework. The SCC captures the cost in dollars of the economic damage that would result from emitting one additional ton of carbon dioxide into the atmosphere. This optimal price of carbon helps decision makers to set the right price of carbon, and serves as a metric to compare models. We first calculate the SCC in the presence of nominal rigidities and then analyze the economic implications of adhering to its trajectory.

6.1. **The social cost of carbon in the presence of sticky prices.** Since our framework is the first integrated assessment model to incorporate price rigidities, our objective is to determine whether nominal rigidities significantly influence the socially optimal carbon price. The Social Cost of Carbon (SCC), defined as the optimal carbon price, can be expressed as:

$$SCC_t = \frac{\beta}{\lambda_t^c}\mathbb{E}_t\left\{\lambda_{t+1}^c SCC_{t+1} + 1000\xi_m l_{t+1} z_{t+1}^{1-\sigma_c}\gamma\frac{\psi}{\alpha}\left(\frac{n_{t+1}}{1-\omega}\right)^{1+\sigma_n}\right\}, \tag{30}$$

where $\gamma \frac{\psi}{\alpha} \left(n_{t+1} / \left(1 - \omega \right) \right)^{1+\sigma_n}$ captures the marginal damage and λ_t^c is the marginal utility of consumption to express the SCC into consumption equivalents. This formulation is quite similar to that of Golosov et al. (2014), where the carbon tax is proportional to output.

If n_{t+1} is derived purely from production, nominal rigidities would not have an impact. However, nominal rigidities directly influence the marginal utility of consumption, which serves as the pricing kernel for wealth. We define the marginal utility of consumption as $\lambda_t^c = \varepsilon_t^b \left(\frac{x_t y_t}{1-\omega} - \omega d_t \right)^{-\sigma_c}$. A persistent gap between realized inflation and the central bank's target $(\pi_t - \pi_t^*)$, driven by climate policies, reduces x_t and diminishes the perceived wealth of economic agents. Consequently, this necessitates a reduction in the stringency of carbon policy and, by extension, a decrease in the social cost of carbon.

FIGURE 7. The social cost of carbon

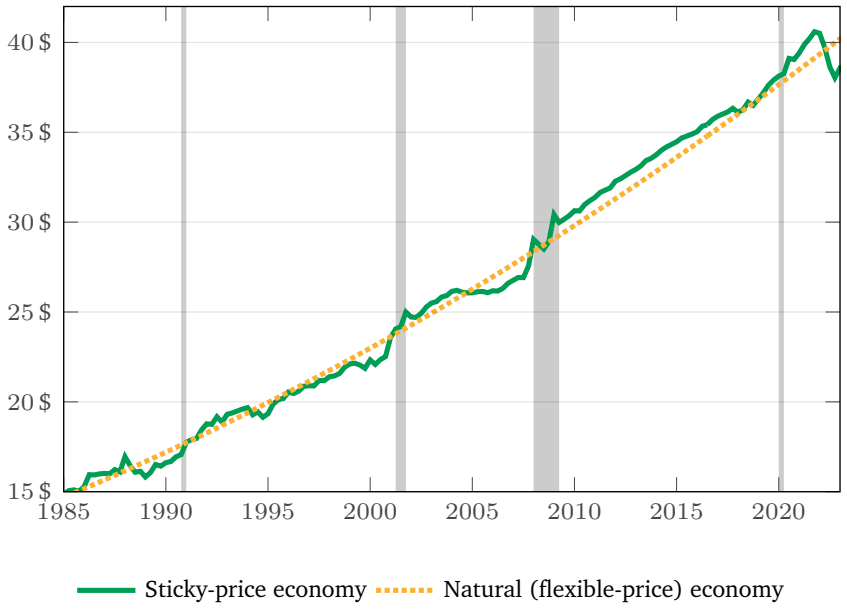

Note: This figure displays the social cost of carbon derived from the estimated New Keynesian Climate model (green line) and its flexible-price (natural) counterpart (yellow dotted line). The grey shaded areas denote the periods of recession as defined by the NBER.

To investigate whether nominal rigidities are sufficiently significant to justify reducing the SCC, we calculate the SCC assuming flexible prices and compare it with its sticky-price counterpart. Figure 7 shows that both SCCs follow the same growth trajectory. The primary differences arise from economic fluctuations, which cause the SCC under nominal rigidities to fluctuate. For instance, the energy price shock following the Ukraine war resulted in a lower SCC owing to the substantial decline in the marginal utility of consumption during the recession. While these rigidities lead to a modest reduction in consumption due to menu costs, the

associated wealth effects on the marginal utility of consumption are minimal. Consequently, the social cost of carbon remains virtually unchanged, underscoring the robustness of the case for ambitious climate policies similar to those advocated in flexible-price settings.

6.2. **The effects of adhering to optimal transition pathways.** We now compare the effects of the Paris Agreement trajectory with those of two optimal carbon pathways: one linked to the SCC and another associated with optimal exhaustion of the carbon budget.

Under the Paris Agreement scenario, the carbon stock will rise from 1036 GtC in 2023 to 1143 GtC by 2050. To facilitate the comparison, we consider a carbon budget of 400 $GtCO_2$, which approximates the difference between the initial and terminal carbon stock values during the transition. Consequently, the carbon budget, denoted by $s_t = 1,143 - m_t$, could be exploited using the following extraction rate:

$$\max_{\{s_t\}} \mathbb{E}_t \left\{ \sum_{s=0}^{\infty} \tilde{\beta}_{t,t+s} \left(\frac{c_{t+s}^{1-\sigma_c} - 1}{1-\sigma_c} - \psi_{t+s} \frac{n_{t+s}^{1+\sigma_n}}{1+\sigma_n} \right) \right\}, \text{ s.t. } \Delta s_t = -\xi_m e_t. \tag{31}$$

This optimal path for s_t represents the optimal exhaustion of the carbon budget and provides an alternative trajectory for the carbon tax.

Figure 8 shows the trajectories of the main variables under the *(i)* Paris Agreement scenario (green line), *(ii)* carbon tax path aligned with the SCC (yellow line), and *(iii)* carbon tax path corresponding to the carbon-budget rule (purple line).

Under the policy implementing the social cost of carbon as the carbon tax, it is optimal to emit 100 GtC more carbon than the level reached under the Paris Agreement. The carbon tax is initially higher upon implementation in 2023 but increases at a relatively slower rate than under the carbon-budget rule or the Paris Agreement. Inflation is initially higher due to the substantial increase in the carbon tax; however, the resulting economic contraction is less severe. Net-zero emissions are achieved in 2075. By contrast, under the carbon-budget rule, it is optimal to reduce carbon emissions more rapidly than under the Paris Agreement. This approach leads to an increase in the carbon tax, higher inflation and nominal interest rates, and more pronounced economic contraction. Consequently, the carbon stock increases at a slower rate.

Contrary to the objectives of the Paris Agreement, the SCC and carbon-budget rule suggest that delaying net-zero emissions beyond 2050 is optimal. This deferment stems from the fact that eliminating the final unit of carbon is the most economically challenging. As a result, the

optimal strategy for planners involves postponing certain carbon emission reductions while anticipating a decrease in abatement expenses. Although climate stabilization is projected to occur by the end of the century, the cumulative carbon emissions remain equivalent to those in the baseline scenario.

FIGURE 8. Alternative carbon tax trajectories

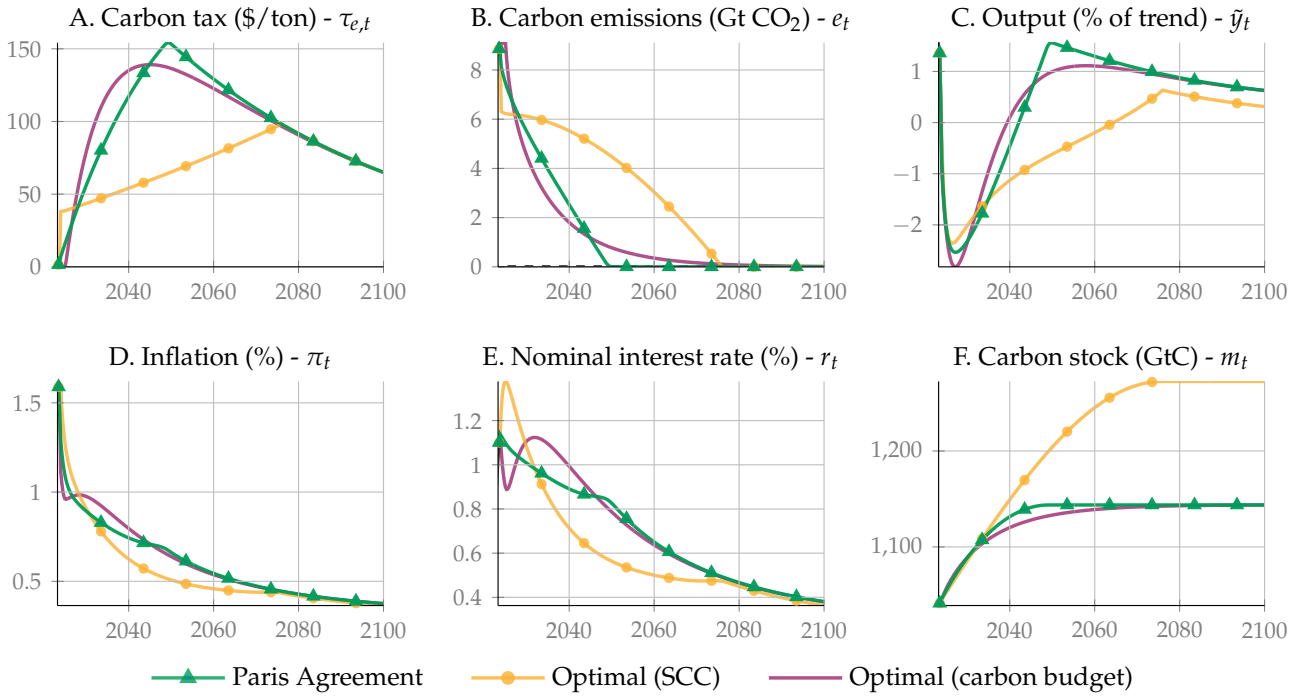

Note: This figure displays the projections of the main variables of the New-Keynesian climate model under two scenarios: *(i)* the Paris Agreement (carbon tax consistent with net zero in 2050) and *(ii)* the optimal tax trajectory (optimal exhaustion of the carbon budget).

7. ROBUSTNESS ANALYSIS

In this final section, we implement three additional exercises to assess the robustness of the primary results. Specifically, we *(i)* introduce sticky wages in addition to sticky prices, *(ii)* modify the redistribution scheme for carbon tax revenue, and *(iii)* include capital in the production function.

7.1. **Sticky wages.** The inflation decomposition in subsection 4.3 highlights that real wages adjust rapidly in response to climate damage. Consequently, we introduce stickiness in wage adjustments to investigate whether this could lead to a greater impact of climate factors and "greenflation" on realized inflation. To this end, we assume that *(i)* the labor market exhibits

monopolistic competition, *(ii)* households delegate salary negotiations to employment agencies in the spirit of Erceg et al. (2000), and *(iii)* there are quadratic costs associated with adjusting nominal wages $W_{i,t}$ for $i \in [0, l_t]$: [24]

$$\mathcal{C}^w_{i,t} = \frac{\kappa_w}{2}\left(\frac{W_{i,t}}{W_{i,t-1}} - \pi^\star_t\right)^2 \frac{W_{i,t}}{P_t} n_{i,t}, \tag{32}$$

where $\kappa_w > 0$ denotes the wage stickiness parameter.

FIGURE 9. The role of wage stickiness

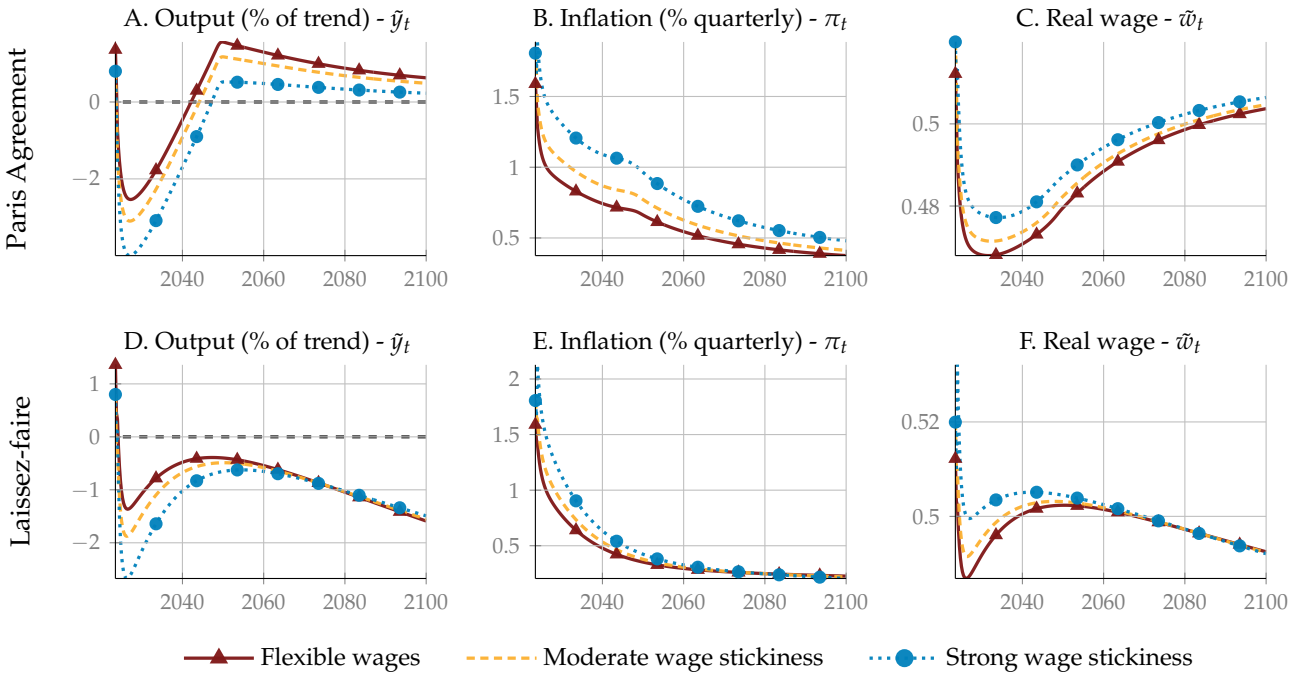

Figure 9 presents the trajectory of key variables under both the Paris Agreement (first row) and laissez-faire (second row) scenarios under different degrees of wage stickiness. In addition to the baseline flexible wage case, two degrees of wage rigidity are considered: pronounced rigidity with $\kappa_w = 20$ and moderate rigidity with $\kappa_w = 10$. Wage stickiness amplifies the inflationary effect and results in a more severe economic contraction by dampening real wage adjustment to the rise in marginal cost due to climate damages and carbon taxes. These results are very much in line with the findings of Olovsson and Vestin (2023) and Del Negro

[24] Each household is a monopolistic supplier of specialized labor $n_{i,t}$. At each point in time t, a large number of competitive "employment agencies" combine households' labor into a homogenous labor input n^d_t sold to firms, according to $n^d_t = (\int_0^1 n_{i,t}^{(\zeta_w-1)/\zeta_w}\,\mathrm{d}i)^{\zeta_w/(\zeta_w-1)}$. Profit maximization by perfectly competitive employment agencies implies the labor demand function $n_{i,t} = (W_{i,t}/W_t)^{-\zeta_w} n^d_t$, where $W_t \equiv (\int_0^1 W_{i,t}{}^{1-\zeta_w}\mathrm{d}i)^{1/(1-\zeta_w)}$ is the nominal wage paid by firms for the homogenous labor input sold to them by agencies. ζ_w is the elasticity of substitution between any two labor types.

et al. (2023), who also find that sticky wages tends to increase inflation during the transition in energy consumption models.

7.2. **Redistribution of carbon tax revenues.** In the baseline scenario, carbon tax revenues are fully redistributed to Ricardian households for simplicity. In this case, the revenues have a minimal impact on consumption, as Ricardian households respond to changes in distorting tax rates and interest rates, but not to lump-sum transfers. However, alternative redistribution schemes can be considered by generalizing the transfer rule as follows:

$$d_{i,t} = z_t l_t \Phi\left(m_t\right) d + \upsilon \frac{T^e_{i,t}}{\omega}, \tag{33}$$

where $\upsilon \in [0,1]$ determines the share of carbon tax revenues redistributed to poor households. The baseline case, denoted as "regressive redistribution", implies $\upsilon = 0$. Alternatively, a "flat transfer" scheme can be assumed where $\upsilon = 1/2$. In this case both types of households receive the same amount. Finally, in the "progressive redistribution" case with $\upsilon = 2/3$ low-productivity households receive twice the amount given to high-productivity households.

Figure 10 illustrates the impact of these three policies under the Paris Agreement scenario. Increasing transfers to low-productivity workers leads to somewhat higher aggregate output and consumption, reducing the cost of carbon pricing policies. At the same time, it also results in higher inflation. In heterogeneous agent models, such as Benmir and Roman (2022), Langot et al. (2023) and Auclert et al. (2023), it has already been found that the redistributional aspects of carbon taxes matter for the transition path. Our simple framework with a fixed fraction of poor households corroborates the importance of the redistribution scheme for inflation dynamics.

FIGURE 10. The role of social transfers during the transition

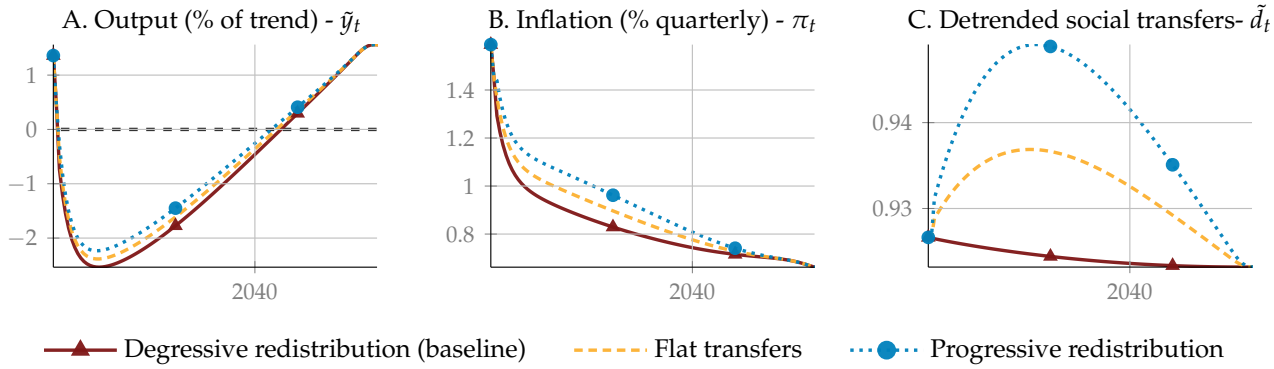

7.3. **Capital in the production function.** Thus far, we have for simplicity considered labor as the sole input in the production function. This allowed us to derive a system of tractable equations as in Woodford (2003). In Integrated Assessment Models (IAMs) like DICE capital plays a more significant role. In this section we therefore investigate whether the green transition is affected by the inclusion of capital.

We introduce capital $k_{j,t}$ in the production function of firm j as follows:

$$y_{j,t} = \Phi(m_t) \left(z_t n_{j,t}^d \right)^{\alpha} k_{j,t-1}^{1-\alpha}. \tag{34}$$

The accumulation of capital is given by $k_{j,t} = (1-\delta) k_{j,t-1} + \left(1 - \mathcal{C}_{j,t}^{\iota}\right) \iota_{j,t}$, where δ is the capital depreciation rate, $\iota_{j,t}$ is investment and $\mathcal{C}_{j,t}^{\iota}$ are investment adjustment costs. These costs are given by $\mathcal{C}_{j,t}^{\iota} = \frac{\kappa_\iota}{2} \left(\frac{\iota_{j,t}}{\iota_{j,t-1}} - g_{z,t} \right)^2$, with κ_ι being a parameter that determines the magnitude of the costs.

Figure 11 illustrates the trajectory of the economy under the Paris Agreement with and without capital. In the latter economy we set $\delta = 0.015$ and $\kappa_\iota = 1$. The green transition results in a strong crowding out of conventional investment, a deeper recession and higher inflation.

FIGURE 11. The role of capital in the production function during the transition

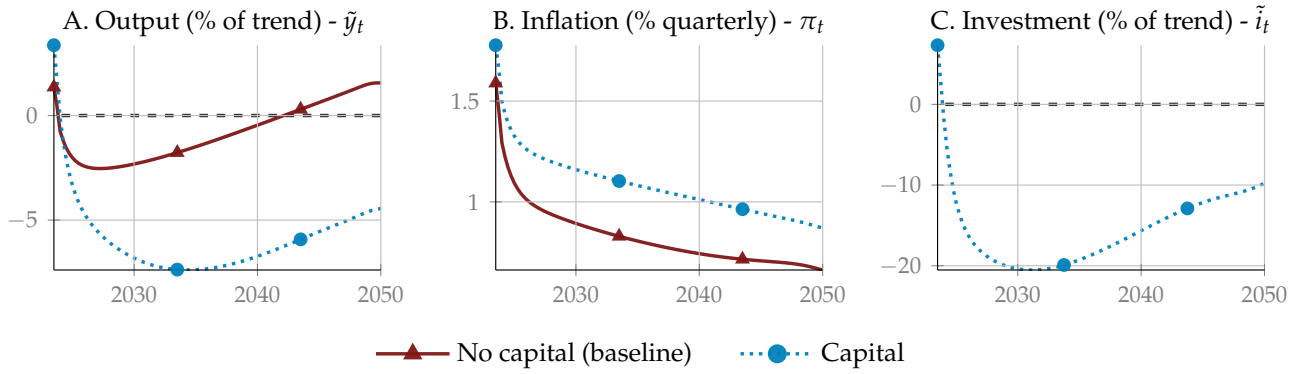

8. CONCLUSION

This paper has developed and analyzed an augmented New Keynesian model that incorporates the trade-off between the short-term cost of mitigation and the long-term cost of global warming. By extending the traditional New Keynesian framework to include carbon stock dynamics, climate externalities and abatement costs, this paper provides a comprehensive framework for understanding the interactions between alternative mitigation policies

and macroeconomic outcomes. Our empirical analysis, based on the Bayesian estimation of a fully nonlinear model, provides a data-grounded quantitative analysis of the transition to a net-zero carbon economy.

We show that under the estimated monetary policy rule mitigation policies that implement the Paris Agreement with rising carbon taxes and increased abatement spending lead to more persistent inflation relative to a laissez-faire environment policy. These results are robust with respect to various alternative specifications of the model and its parameters. However, the short-term costs of the green transition, characterized by heightened dispersion in inflation and output, must be balanced against the long-term benefits of lower damages from climate change to productivity and higher output and consumption. Monetary policy rules that integrate the rise in the natural rate of interest due to the abatement spending are able to mitigate the inflationary effects of carbon taxes. Finally, we find that the social cost of carbon is largely unaffected by sticky prices. Although these rigidities slightly reduce consumption, they do not significantly alter the transition trajectory.

References

Adjemian, S. and Juillard, M. (2014). Assessing long run risk in a DSGE model under ZLB with the stochastic extended path approach. *Mimeo*, CEPREMAP.

Adjemian, S., Juillard, M., Karamé, F., Mutschler, W., Pfeifer, J., Ratto, M., Rion, N., and Villemot, S. (2024). Dynare: Reference manual, version 6. *Dynare Working Paper #80*, CEPREMAP.

Aguiar, M. and Gopinath, G. (2007). Emerging market business cycles: The cycle is the trend. *Journal of political Economy*, 115(1):69–102.

An, S. and Schorfheide, F. (2007). Bayesian analysis of DSGE models. *Econometric Reviews*, 26:113–172.

Annicchiarico, B., Correani, L., and Di Dio, F. (2018). Environmental policy and endogenous market structure. *Resource and Energy Economics*, 52:186–215.

Annicchiarico, B. and Di Dio, F. (2015). Environmental policy and macroeconomic dynamics in a New Keynesian model. *Journal of Environmental Economics and Management*, 69:1–21.

Annicchiarico, B. and Di Dio, F. (2017). GHG emissions control and monetary policy. *Environmental & Resource Economics*, 67:823–851.

Atkinson, T., Richter, A., and Throckmorton, N. (2020). The zero lower bound and estimation accuracy. *Journal of Monetary Economics*, 115:249–264.

Auclert, A., Monnery, H., Rognlie, M., and Straub, L. (2023). Managing an energy shock: Fiscal and monetary policy. *Working Paper #31543*, National Bureau of Economic Research.

Barrage, L. and Nordhaus, W. (2024). Policies, projections, and the social cost of carbon: Results from the dice-2023 model. *Proceedings of the National Academy of Sciences*, 121(13):e2312030121.

Benigno, P. and Eggertsson, G. B. (2023). It's baaack: The surge in inflation in the 2020s and the return of the non-linear Phillips curve. *Working Paper #31197*, National Bureau of Economic Research.

Benmir, G., Jaccard, I., and Vermandel, G. (2020). Green asset pricing. *Working Paper #2477*, European Central Bank.

Benmir, G. and Roman, J. (2022). The distributional costs of net-zero: A hank perspective. *Mimeo*, London School of Economics.

Bilbiie, F., Ghironi, F., and Melitz, M. (2012). Endogenous entry, product variety, and business cycles. *Journal of Political Economy*, 120:304–345.

Carattini, S., Heutel, G., and Melkadze, G. (2023). Climate policy, financial frictions, and transition risk. *Review of Economic Dynamics*, 51:778–794.

Chow, G. C. and Lin, A.-L. (1971). Best linear unbiased interpolation, distribution, and extrapolation of time series by related series. *The Review of Economics and Statistics*, 53:372–375.

Christiano, L., Motto, R., and Rostagno, M. (2014). Risk shocks. *American Economic Review*, 104:27–65.

Clarida, R., Gali, J., and Gertler, M. (1999). The science of monetary policy: a new keynesian perspective. *Journal of economic literature*, 37:1661–1707.

Coenen, G., Lozej, M., and Priftis, R. (2024). Macroeconomic effects of carbon transition policies: an assessment based on the ECB's new area-wide model with a disaggregated energy sector. *European Economic Review*, 167:104798.

Cuba-Borda, P., Guerrieri, L., Iacoviello, M., and Zhong, M. (2019). Likelihood evaluation of models with occasionally binding constraints. *Journal of Applied Econometrics*, 34:1073–1085.

Del Negro, M., di Giovanni, J., and Dogra, K. (2023). Is the green transition inflationary? *Staff Reports #1053*, Federal Reserve Bank of New York.

Del Negro, M., Giannoni, M. P., and Patterson, C. (2023). The forward guidance puzzle. *Journal of Political Economy Macroeconomics*, 1(1):43–79.

Del Negro, M., Giannoni, M. P., and Schorfheide, F. (2015). Inflation in the great recession and new keynesian models. *American Economic Journal: Macroeconomics*, 7:168–196.

Diluiso, F., Annicchiarico, B., Kalkuhl, M., and Minx, J. (2021). Climate actions and macro-financial stability: The role of central banks. *Journal of Environmental Economics and Management*, 110.

Erceg, C. J., Henderson, D. W., and Levin, A. T. (2000). Optimal monetary policy with staggered wage and price contracts. *Journal of Monetary Economics*, 46:281–313.

Fair, R. and Taylor, J. (1983). Solution and maximum likelihood estimation of dynamic nonlinear rational expectations models. *Econometrica*, 51:1169–1185.

Fernández-Villaverde, J., Gillingham, K., and Scheidegger, S. (2024). Climate change through the lens of macroeconomic modeling. *Working Paper #32963*, National Bureau of Economic Research.

Fernández-Villaverde, J., Rubio-Ramírez, J. F., and Schorfheide, F. (2016). Solution and estimation methods for DSGE models. In *Handbook of Macroeconomics*, volume 2, pages 527–724. Elsevier.

Ferrari, A. and Nispi Landi, V. (2024). Will the green transition be inflationary? Expectations matter. *IMF Economic Review*, pages 1–64.

Fève, P., Matheron, J., and Sahuc, J.-G. (2010). Inflation target shocks and monetary policy inertia in the euro area. *The Economic Journal*, 120:1100–1124.

Finkelstein Shapiro, A. and Metcalf, G. E. (2023). The macroeconomic effects of a carbon tax to meet the US Paris Agreement target: The role of firm creation and technology adoption. *Journal of Public Economics*, 218:104800.

Galí, J. (2015). *Monetary policy, inflation, and the business cycle: an introduction to the new Keynesian framework and its applications*. Princeton University Press.

Gibson, J. and Heutel, G. (2023). Pollution and labor market search externalities over the business cycle. *Journal of Economic Dynamics and Control*, 151:104665.

Golosov, M., Hassler, J., Krusell, P., and Tsyvinski, A. (2014). Optimal taxes on fossil fuel in general equilibrium. *Econometrica*, 82:41–88.

Guerrieri, L. and Iacoviello, M. (2017). Collateral constraints and macroeconomic asymmetries. *Journal of Monetary Economics*, 90:28–49.

Harding, M., Lindé, J., and Trabandt, M. (2023). Understanding post-covid inflation dynamics. *Journal of Monetary Economics*, 140:S101–S118.

Hazell, J., Herreno, J., Nakamura, E., and Steinsson, J. (2022). The slope of the phillips curve: evidence from us states. *The Quarterly Journal of Economics*, 137(3):1299–1344.

Heutel, G. (2012). How should environmental policy respond to business cycles? Optimal policy under persistent productivity shocks. *Review of Economic Dynamics*, 15:244–264.

Holston, K., Laubach, T., and Williams, J. C. (2017). Measuring the natural rate of interest: International trends and determinants. *Journal of International Economics*, 108:S59–S75.

IPCC (2021). Climate change 2021: The physical science basis.summary for policymakers. Contribution of Working Group I to the Sixth Assessment Report of the Intergovernmental Panel on Climate Change.

Ireland, P. N. (2007). Changes in the federal reserve's inflation target: Causes and consequences. *Journal of Money, Credit and Banking*, 39:1851–1882.

Jo, A. and Miftakhova, A. (2024). How constant is constant elasticity of substitution? Endogenous substitution between clean and dirty energy. *Journal of Environmental Economics and Management*, 125:102982.

Jondeau, E., Levieuge, G., Sahuc, J.-G., and Vermandel, G. (2023). Environmental subsidies to mitigate net-zero transition costs. *Working Paper #910*, Banque de France.

Juillard, M. (1996). Dynare: A program for the resolution and simulation of dynamic models with forward variables through the use of a relaxation algorithm. *Working Paper #9602*, CEPREMAP.

Langot, F., Malmberg, S., Tripier, F., and Hairault, J.-O. (2023). The macroeconomic and redistributive effects of shielding consumers from rising energy prices: A real time evaluation of the french experiment. *Working Paper #2305*, CEPREMAP.

Laubach, T. and Williams, J. C. (2003). Measuring the natural rate of interest. *Review of Economics and Statistics*, 85(4):1063–1070.

McKay, A., Nakamura, E., and Steinsson, J. (2017). The discounted Euler equation: A note. *Economica*, 84:820–831.

Nakov, A. and Thomas, C. (2023). Climate-conscious monetary policy. *Working Paper #2845*, European Central Bank.

Nordhaus, W. (1992). The 'DICE' model: Background and structure of a dynamic integrated climate-economy model of the economics of global warming. *Technical Report*, Cowles

Foundation for Research in Economics, Yale University.

Nordhaus, W. D. (2017). Revisiting the social cost of carbon. *Proceedings of the National Academy of Sciences*, 114:1518–1523.

Nuño, G., Renner, P., and Scheidegger, S. (2024). Monetary policy with persistent supply shocks. *Available at SSRN*.

OECD (2017). Entrepreneurship at a Glance. *OECD Publishing*.

Olovsson, C. and Vestin, D. (2023). Greenflation? *Working Paper #420*, Sveriges Riksbank.

Orphanides, A. (2002). Monetary-policy rules and the great inflation. *American economic review*, 92(2):115–120.

Pappa, E., Airaudo, F., and Seoane, H. D. (2023). The green metamorphosis of a small open economy. *Discussion Paper #17863*, Centre for Economic Policy Research.

Schnabel, I. (2022). A new age of energy inflation: climateflation, fossilflation and greenflation. In *Remarks at a panel on Monetary Policy and Climate Change at The ECB and its Watchers XXII Conference, Frankfurt am Main*, volume 17.

Smets, F. and Wouters, R. (2003). An estimated dynamic stochastic general equilibrium model of the euro area. *Journal of the European economic association*, 1(5):1123–1175.

Smets, F. and Wouters, R. (2007). Shocks and frictions in US business cycles: A Bayesian DSGE approach. *American Economic Review*, 97:586–606.

Woodford, M. (2003). *Interest and prices*. Princeton University Press.

APPENDIX A. FULL MODEL

This appendix presents the full set of equations. It includes four core equations and variables $\{\tilde{y}_t, \pi_t, r_t, \tilde{m}_t\}$:

$$\left(\frac{x_t\tilde{y}_t - \omega\tilde{d}_t}{1-\omega}\right)^{-\sigma_c} = \beta\mathbb{E}_t\left\{\frac{\varepsilon_{b,t+1}}{\varepsilon_{b,t}}\frac{r_t}{\pi_{t+1}}\left((1-\omega)\left(\frac{x_{t+1}\tilde{y}_{t+1} - \omega\tilde{d}_t}{1-\omega}\right)^{-\sigma_c} + \omega\tilde{d}_t{}^{-\sigma_c}\right)\right\} \tag{A.1}$$

$$(\pi_t - \pi_t^\star)\,\pi_t = (1-\vartheta)\beta\mathbb{E}_t\left\{(1+g_{z,t+1})\,\frac{\tilde{y}_{t+1}}{\tilde{y}_t}\,(\pi_{t+1} - \pi_{t+1}^\star)\,\pi_{t+1}\right\} + \frac{\zeta}{\kappa}\varepsilon_{p,t}mc_t + \frac{1-\zeta}{\kappa} \tag{A.2}$$

$$\frac{r_t}{r} = \left(\frac{r_{t-1}}{r}\right)^\rho\left[\left(\frac{\pi_t^\star}{\pi}\right)\left(\frac{\pi_t}{\pi_t^\star}\right)^{\phi_\pi}\left(\frac{\tilde{y}_t}{\tilde{y}_t^n}\right)^{\phi_y}\right]^{1-\rho}\varepsilon_t^r \tag{A.3}$$

$$\tilde{m}_t = (1-\delta_m)\tilde{m}_{t-1} + \xi_m\sigma_t\left(1 - \tilde{\tau}_{e,t}^{\frac{1}{\theta_2-1}}\right)z_t l_t\tilde{y}_t\varepsilon_{e,t} \tag{A.4}$$

The model also includes auxiliary variables:

$$x_t = 1 - (1-\vartheta)\frac{\kappa}{2}(\pi_t - \pi_t^\star)^2 - \theta_{1,t}\tilde{\tau}_{e,t}^{\theta_2/(\theta_2-1)} - \vartheta(1 - \epsilon_{p,t}mc_t) \tag{A.5}$$

$$mc_t = \frac{\psi}{\epsilon_{b,t}(1-\omega)^{\sigma_c+\sigma_n}}\frac{\left(x_t\tilde{y}_t - \omega\tilde{d}_t\right)^{\sigma_c}\tilde{y}_t^{\sigma_n}}{\Phi\left(\tilde{m}_t\right)^{1+\sigma_n}} + \theta_{1,t}\tilde{\tau}_{e,t}\left[\theta_2 + (1-\theta_2)\,\tilde{\tau}_{e,t}^{\frac{1}{\theta_2-1}}\right] \tag{A.6}$$

where $\tilde{y}_t = y_t/(z_t l_t y)$, $\tilde{d}_t = d_t/z_t$, $\tilde{\tau}_{e,t} = \tau_{e,t}\sigma_t\varepsilon_{e,t}/(\theta_2\theta_{1,t})$, and $\tilde{m}_t = m_t - m_{1750}$.

Finally, it comprises five trend related deterministic processes

$$\sigma_t = \sigma_{t-1}(1-g_{\sigma,t}) \quad \text{and} \quad g_{\sigma,t} = (1-\delta_\sigma)\,g_{\sigma,t-1}, \tag{A.7}$$

$$z_t = z_{t-1}(1+g_{z,t}) \quad \text{and} \quad g_{z,t} = g_{z,t-1}\,(1-\delta_z)\,, \tag{A.8}$$

$$\theta_{1,t} = (p_b/\theta_2)(1-\delta_{pb})^{t-t_0}\sigma_t, \tag{A.9}$$

$$l_t = l_{t-1}\,(l_T/l_{t-1})^{\ell_g}\,, \tag{A.10}$$

$$\pi_t^\star = (1-\rho_{\pi^\star})\,\pi + \rho_{\pi^\star}\pi_{t-1}^\star + \eta_{\pi^\star,t}, \tag{A.11}$$

and four stochastic processes:

$$\varepsilon_{b,t} = (1-\rho_b) + \rho_b\varepsilon_{b,t-1} + \eta_{b,t}; \quad \varepsilon_{p,t} = (1-\rho_p) + \rho_p\varepsilon_{p,t-1} + \eta_{p,t};$$

$$\varepsilon_{e,t} = (1-\rho_e) + \rho_e\varepsilon_{e,t-1} + \eta_{e,t}; \quad \varepsilon_{r,t} = (1-\rho_r) + \rho_r\varepsilon_{r,t-1} + \eta_{r,t}.$$

APPENDIX B. THE EXTENDED PATH APPROACH

A perfect foresight algorithm typically requires *(i)* a finite number of periods and *(ii)* a terminal period to compute each endogenous variable in order to realize economic surprises. To fix notation, this general representation in the presence of extended path takes the form:

$$\tilde{y}_t = g_\Theta\left(y_0, y, 0\right) \tag{B.1}$$

$$y_t = \mathbb{E}_{t,t+S}\left\{g_\Theta\left(y_{t-1}, \tilde{y}_{t+S+1}, \varepsilon_t\right)\right\} \tag{B.2}$$

$$\mathcal{Y}_t = h_\Theta\left(y_t\right) \tag{B.3}$$

$$\varepsilon_t \sim \mathcal{N}\left(0, \Sigma_\varepsilon\right) \tag{B.4}$$

The first equation determines the deterministic evolution of the endogenous variables in the absence of shocks summarized in vector $\tilde{y}_t$ with initial conditions y_0 and terminal (asymptotic) state y for a given set of nonlinear equations $g_\Theta(\cdot)$. The second equation determines the path of endogenous variables y_t with economic surprise, ε_t is a vector of exogenous stochastic innovations that are normally distributed with mean zero and covariance Σ_ε; Θ is the vector of structural parameters; $h_\Theta(\cdot)$ and $g_\Theta(\cdot)$ are the set of nonlinear equations. $\mathbb{E}_{t,t+S}\{\cdot\}$ is the extended path-consistent expectation operator, which updates expectations over a specific time horizon of size S, and takes as given $\tilde{y}_{t+S+1}$ the terminal period of the expectation. Therefore, the size of the expectation window S must be sufficiently large to ensure that the value of $\tilde{y}_{t+S+1}$ does not affect the outcome. [25] The third equation relates the observations summarized in the vector $\mathcal{Y}_t$ to the endogenous variables in y_t. The last equation concerns the distribution of exogenous innovations.

For each evaluation of the sample likelihood, we first compute the deterministic path providing the transition between the initial period $\{\tilde{y}_t\}_{t=1}^{T}$ and the terminal period. We select a value of $T = 1,000$ to allow convergence to the terminal state. Formally, we use Equation B.1 assuming that (*i*) no shock with sequence $\{\varepsilon_t\}_{t=1}^{T}$ is all zeros, and (*ii*) a terminal condition that is the steady state of the model $\tilde{y}_{t+S+1} = y$, which can be written as $\tilde{y}_t = g_\Theta\left(y_{t_0}, y, 0\right)$. Next, we use the inversion filter to find the sequence of $\{\varepsilon_t\}_{t=1}^{T^*}$ that matches sample $\{\mathcal{Y}_t\}_{t=1}^{T^*}$ with T^* observations using $\{\tilde{y}_t\}_{t=1}^{T}$ as the terminal value of the expectation window. This

[25] One must strike a balance between the length of the expectation window to mimic infinite-horizon rational expectations, and the computational burden of updating the expectations. We select an expectation horizon of 40 years ($S = 160$). This length is sufficiently large to ensure that the terminal conditions do not quantitatively affect the numerical value of the likelihood function, but exhibits a moderate computational burden.

implicitly assumes that agents expect the economy to return to its deterministic path $\tilde{y}$ after S periods. Based on the smoothed sequence $\{\varepsilon_t\}_{t=1}^{T^*}$, the likelihood function $\mathcal{L}(\theta, \mathcal{Y}_{1:T^*})$ of the model is obtained, conditional on the matrix of observations through time T^*.

APPENDIX C. MODEL EVALUATION

The quality of the model is first assessed by comparing the data and model-implied moments, as listed in Table C.1. Data moments are computed for 1985Q1-2023Q2. Model-implied moments are reported with their 90% confidence intervals, based on 1000 random draws from the parameter distributions. Table C.1 shows that the model reproduces the main data statistics relatively well, despite its small size.

TABLE C.1. Empirical and model-implied moments

	DATA	MODEL [5%;95%]	DATA	MODEL [5%;95%]
	Mean		**Standard deviations**	
Output growth	0.007	[0.007;0.008]	0.012	[0.011;.0.015]
Inflation rate	0.011	[0.000;0.016]	0.007	[0.005;0.012]
Nominal interest rate	0.008	[-0.001;0.017]	0.006	[0.004;0.013]
Carbon emission growth	0.004	[0.003;0.004]	0.013	[0.012;0.016]
	Autocorrelation		**Correlation w/ output**	
Output growth	-0.199	[-0.239;0.054]	1.000	[1.000;1.000]
Inflation rate	0.977	[0.835;0.976]	0.204	[-0.177;0.234]
Nominal interest rate	0.988	[0.967;0.996]	-0.038	[-0.175;0.236]
Carbon emission growth	-0.100	[-0.224;-0.064]	0.965	[0.877;0.945]

Note: Model-implied moments are computed across 1,000 random artificial series, each of the same size as the data sample.

Indeed, the model's performance is relatively good compared to the usual standards in the inference of real business cycle models. Specifically, the model accurately replicates the volatility of inflation and the nominal interest rate. However, it tends to underestimate the volatility of output and carbon emissions, suggesting a potential area for improvement. First-order autocorrelations are also successfully matched, with the exception of inflation which is found to be weaker in the model. Regarding the cross-correlation with output, the model performs well, accurately capturing the relationship between output and most variables, except for carbon emission growth. This suggests that further refinement or adjustments may be required to better align the model's representation of carbon emission growth with the observed patterns.

Second, the model is evaluated based on impulse response functions (IRFs). IRFs are useful for assessing how shocks to economic variables reverberate through economic and climate systems. Figure C.1 reports the generalized impulse response functions of the estimated model taking the parameters at their posterior mode among metropolis-hasting draws.

FIGURE C.1. Generalized impulse response functions of the estimated model

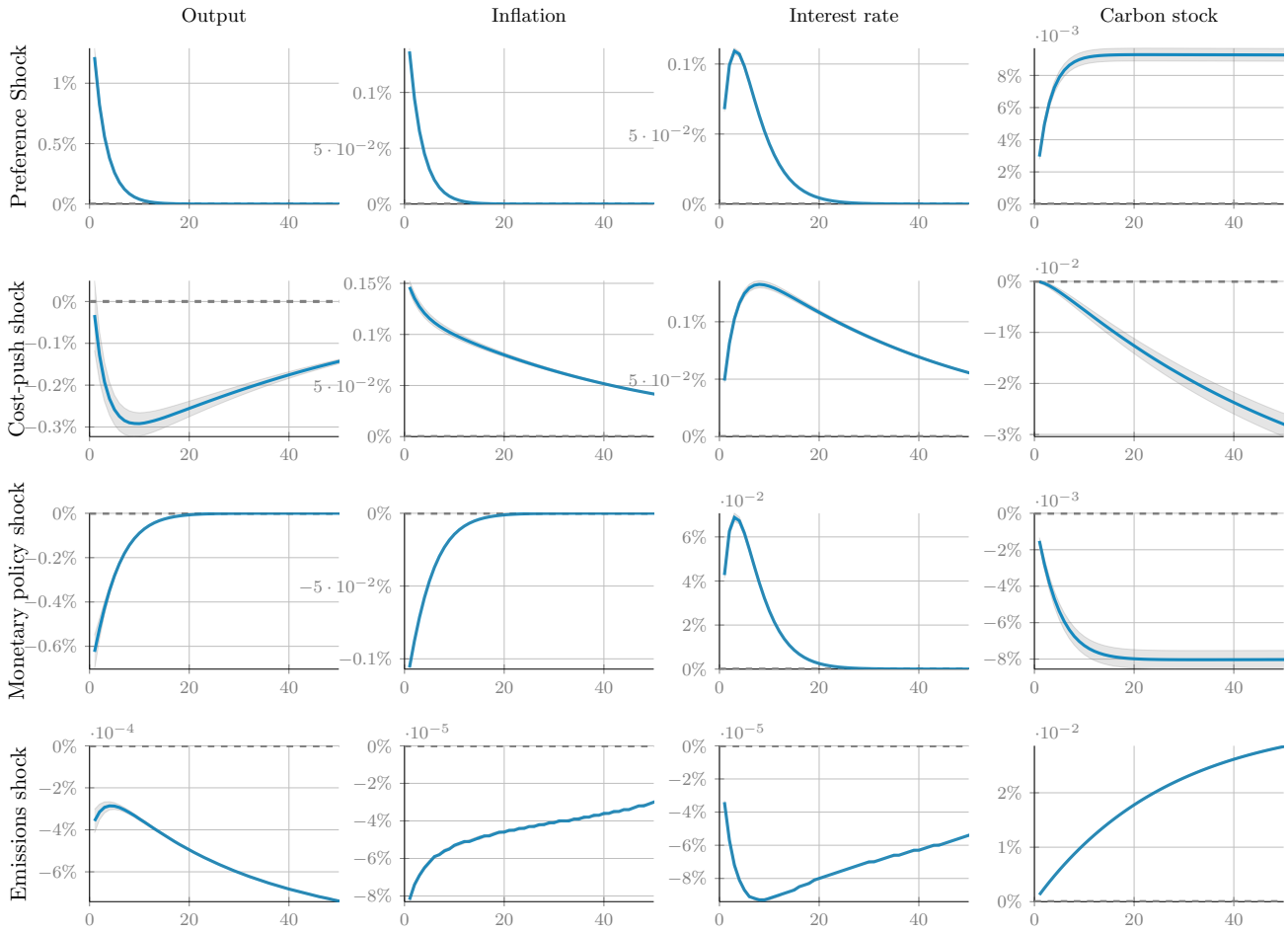

Note: The figure displays the generalized impulse response functions (GIRFs) of several variables for four shocks: preference, cost-push, monetary policy, and emissions in lines 1 to 4, respectively. The GIRFs are computed using the value of the state variables in 2023Q2, and each GIRF is expressed as a percentage deviation from its initial value in 2023. GIRFs are averaged based on 500exogenous draws.

The first row of Figure C.1 displays the responses to a positive preference shock that boosts household consumption. In response, the aggregate output increases, reflecting the positive impact of increased wealth on overall economic activity. This increase in output leads to a corresponding rise in both the inflation rate and the carbon stock. To counteract the inflationary effect of this positive demand shock, the interest rate increases, creating a modest recession when the shock process has decayed sufficiently.

The second row of Figure C.1 reports the responses of the economy to the cost-push shock, similar to the markup shock of Smets and Wouters (2007). This supply shock increases firms' selling price and is detrimental to the rest of the economy. The central bank must strike a balance between price and quantity stabilization, because the interest rate cannot stabilize when these two variables are in opposite directions. The real interest rate increases slightly following the realization of the shock which reduces output with a delay. Notably, the reduction in output also has a positive consequence in terms of emissions: there is a corresponding decrease in production and economic activity, resulting in reduced emissions.

The third row of Figure C.1 shows the responses to a monetary policy shock. This shock is interpreted as a temporary deviation of the nominal rate from the systematic component of the policy rule. By boosting the return on safe assets, this shock reduces the willingness to consume and depresses aggregate demand. This decline in aggregate demand forces firms to reduce hourly demand. The equilibrium wage clearing the labor market declines, thus creating a joint decline in the marginal cost and selling price of the goods. This decline in quantity also reduces emissions and makes the carbon stock lower than expected.

The last shock is the emission intensity shock, which materializes as an exogenous increase in carbon emissions. This shock increases the carbon stock in the atmosphere and causes modest economic damage. However, its effects on inflation and interest rates are too small to measure.

Finally, Figure C.2 provides an interpretation of the historical fluctuations of output, inflation and the nominal interest rate through the lens of the identified structural shocks of the New Keynesian climate model.

FIGURE C.2. Historical decomposition of detrended output, inflation and the nominal interest rate on the sample period

Note: This figure displays the approximate contribution of each shock to the determination of the variable of interest. The cross-products across the contribution of shocks are neglected.

APPENDIX D. MATH DERIVATIONS

This appendix provides additional details on the decomposition of output and inflation.

D.1. **Demand part.** Detrended Euler equation reads as:

$$\tilde{\lambda}_t = \mathbb{E}_t \left\{ \beta \frac{r_t}{\pi_{t+1}} \left((1-\omega)\tilde{\lambda}_{t+1} + \omega \varepsilon_{b,t+1} \tilde{d}_t^{\,-\sigma_c} \right) \right\}. \tag{D.1}$$

It can be rewritten as:

$$\begin{aligned} \tilde{\lambda}_t &= \mathbb{E}_t \left\{ R_t \left((1-\omega)\tilde{\lambda}_{t+1} + \omega \varepsilon_{b,t+1} \tilde{d}_t^{\,-\sigma_c} \right) \right\} \\ &= \omega \mathbb{E}_t \left\{ \sum_{s=0}^{\infty} (1-\omega)^s \, \varepsilon_{b,t+s} \tilde{d}_{t+s}^{-\sigma_c} \prod_{j=0}^{s} R_{t+j} \right\}, \end{aligned}$$

where $R_t = \beta r_t / \pi_{t+1}$.

Recall that: $\tilde{\lambda}_t = \varepsilon_{b,t} \left(\frac{\tilde{c}_t - \omega \tilde{d}_t}{1-\omega} \right)^{-\sigma_c}$, the Euler equation becomes:

$$\left(\frac{c_t/z_t - \omega \tilde{d}_t}{(1-\omega)} \right)^{-\sigma_c} = \omega \mathbb{E}_t \left\{ \sum_{s=0}^{\infty} (1-\omega)^s \, \varepsilon_{b,t+s} \tilde{d}_{t+s}^{-\sigma_c} \prod_{j=0}^{s} R_{t+j} \right\}$$

which can be rewritten as:

$$c_t/z_t = IS_t,$$

where $IS_t = \omega \tilde{d}_t + (1-\omega) \left[\omega \mathbb{E}_t \left\{ \sum_{s=0}^{\infty} \beta \, (1-\omega)^s \, \varepsilon_{b,t+s} \tilde{d}_{t+s}^{-\sigma_c} \prod_{j=0}^{s} \frac{r_{t+j}}{\pi_{t+1+j}} \right\} \right]^{-1/\sigma_c}$.

In addition, we know that:

$$IS_t = c_t/z_t = x_t y_t / (z_t l_t),$$

where $x_t = 1 - (1-\vartheta)\frac{\kappa}{2} (\pi_t - \pi_t^\star)^2 - \theta_{1,t} \tilde{\tau}_{e,t}^{\theta_2/(\theta_2-1)} - \vartheta(1 - \epsilon_{p,t} mc_t)$, with $\mu_t = \tilde{\tau}_{e,t}^{1/(\theta_2-1)}$.

As $c_t = x_t y_t / l_t$, it comes:

$$IS_t = x_t \tilde{y}_t.$$

Therefore, applying the logarithm yields:

$$\hat{y}_t \simeq \widehat{IS}_t + \theta_{1,t} \tilde{\tau}_{e,t}^{\theta_2/(\theta_2-1)} + (1-\vartheta)\frac{\kappa}{2} (\pi_t - \pi_t^*)^2 + \vartheta(1 - \epsilon_{p,t} mc_t),$$

with $\hat{y}_t = \log(\tilde{y}_t/\tilde{y})$ and $\widehat{IS}_t = \log(IS_t/IS)$.

D.2. **Supply part.** The marginal cost is given by:

$$mc_t = \frac{w_t}{\Gamma_t} + \theta_{1,t} \mu_t^{\theta_2} + \tau_{e,t} \sigma_t \, (1 - \mu_t) \, \varepsilon_{e,t}$$

Let us consider the real wage of the high productive worker $w_t = \psi_t n_t^{\sigma_n}/\lambda_t$, the general equilibrium condition $(1-\omega)\, n_t = n_t^d = N_t$ and the production function $y_t = l_t \Gamma_t N_t^{\alpha}$, we obtain:

$$mc_t = \frac{1}{\lambda_t \Gamma_t} \psi_t \left(\left(\frac{y_t}{l_t \Gamma_t} \right)^{\frac{1}{\alpha}} \frac{1}{1-\omega} \right)^{\sigma_n} + \theta_{1,t} \mu_t^{\theta_2} + \tau_{e,t} \sigma_t \left(1-\mu_t\right) \varepsilon_{e,t}$$

Recall that $\Gamma_t = \Phi\left(\tilde{m}_t\right) z_t$ and $\tilde{y}_t = y_t/\left(l_t z_t\right)$, thus:

$$mc_t = \frac{1}{\lambda_t \Phi\left(\tilde{m}_t\right)} \psi z_t^{-\sigma_c} \left(\left(\frac{\tilde{y}_t}{\Phi\left(\tilde{m}_t\right)} \right)^{\frac{1}{\alpha}} \frac{1}{1-\omega} \right)^{\sigma_n} + \theta_{1,t} \mu_t^{\theta_2} + \tau_{e,t} \sigma_t \left(1-\mu_t\right) \varepsilon_{e,t}$$

Next, replacing λ_t by its expression in function of $\tilde{c}_t$ gives:

$$mc_t = \frac{\psi}{\varepsilon_{b,t} \left(\frac{\tilde{c}_t - \omega \tilde{d}_t}{1-\omega} \right)^{-\sigma_c} \Phi\left(\tilde{m}_t\right)} \left(\left(\frac{\tilde{y}_t}{\Phi\left(\tilde{m}_t\right)} \right)^{\frac{1}{\alpha}} \frac{1}{1-\omega} \right)^{\sigma_n} + \tilde{\tau}_{e,t} \theta_{1,t} \left(\theta_2 + \tilde{\tau}_{e,t}^{\frac{1}{\theta_2 - 1}} \left(1-\theta_2\right) \right).$$

Finally,

$$mc_t = \frac{\psi}{\left(1-\omega\right)^{\sigma_c + \sigma_n}} \frac{\left(x_t \tilde{y}_t - \omega \tilde{d}_t\right)^{\sigma_c} \tilde{y}_t^{\frac{\sigma_n}{\alpha}}}{\varepsilon_{b,t} \Phi\left(\tilde{m}_t\right)^{1+\frac{\sigma_n}{\alpha}}} + \tilde{\tau}_{e,t} \theta_{1,t} \left(\theta_2 + \tilde{\tau}_{e,t}^{\frac{1}{\theta_2 - 1}} \left(1-\theta_2\right) \right).$$

Consequently, the Phillips curve is simply the discounted sum of future marginal costs:

$$\pi_t = \frac{\zeta}{\kappa} \mathbb{E}_t \sum_{s=0}^{\infty} \hat{\beta}_{t,t+s} \left[\varepsilon_{p,t+s} mc_{t+s} + \frac{1-\zeta}{\zeta} \right],$$

with $\hat{\beta}_{t,t+s} = \beta^s \frac{y_{t+s} l_t}{y_t l_{t+s}} \frac{1}{\pi_t - \pi_t^{\star}}$.

Appendix E. Sensitivity analysis

This appendix proposes a sensitivity analysis to examine the effects of various structural parameters on inflation and output dynamics during the green transition.

E.1. **The role of attenuated expectations.** The forward guidance puzzle found in the New Keynesian models highlights the issue that the model predicts unrealistically large effects of future policy announcements on current economic outcomes, leading to implausibly strong responses in output and inflation. An announced carbon tax creates a similar effect because it leads to disproportionately large anticipatory changes in current economic behavior, such as investment and consumption, based on the expectation of future policy impacts. Therefore, we examine the sensitivity of our model to this puzzle. Our model comprises two main parameters on the Euler equation and Phillips curve that attenuate the effect of forward real

rates and marginal costs on current outcomes. Panel A of Figure E.1 shows the average values of inflation, output, interest rate, and real rate under the alternative attenuation levels. Attenuation by more intense discounting of the future marginal utilities of consumption tends to increase inflation. By weighting future high real interest rates relatively less, households tend to consume more during the transition, which translates into higher inflation through the demand effect. By contrast, greater discounting makes the Phillips curve less sensitive to future increases in the carbon tax, resulting in relatively lower inflation with the degree of attenuation. Because the economy is less inflationary, it yields a higher output on average during the transition.

E.2. **The Taylor rule.** An additional question pertains to whether the monetary policy stance of a central bank, characterized as dovish or hawkish, exerts influence during the transition period. To determine, we vary the coefficients of the Taylor rule by exploring a relatively higher coefficient on inflation $\phi_\pi \in [1.15, 2]$ and output $\phi_y \in [0.1, 1]$. Panel B of Figure E.1 reports the outcome. We obtain the typical stabilization mechanism: an increase in inflation (resp. output gap) coefficient reduces average inflation (resp. detrended output) during the transition. However, the effects are limited because an increase in the coefficient does not necessarily yield a substantial decrease in the average value of the targeted variable. This finding suggests that the usual trade-off between output and inflation, as discussed by Clarida et al. (1999) and Woodford (2003), does not emerge strongly. It is also noteworthy that the divine coincidence principle, characterized by a situation in which stabilizing inflation also naturally stabilizes the output gap, does not hold true. Indeed, an increase in the output gap coefficient does not reduce inflation, suggesting that the transition is similar to a supply-side phenomenon.

E.3. **Slopes of aggregate demand and supply curves.** Recent literature, such as Hazell et al. (2022), has shown that the New Keynesian Phillips curve has been relatively flat since the 1980s. However, the recent surge in inflation has led to a substantial revision of the price-setting mechanism to accommodate the observed increase in inflation following the Ukrainian war, resulting in a much steeper New Keynesian Phillips curve (e.g., Harding et al., 2023, Benigno and Eggertsson, 2023). Consequently, we assess the sensitivity of our results to adjustments in the slope of the Phillips curve, by altering the Rotemberg coefficient from 50 to 120. Similarly, we investigate the role of the risk aversion coefficient in the household utility

function. In a New Keynesian framework, higher risk aversion dampens the transmission mechanism of monetary policy by making households less responsive to changes in interest rates, thereby reducing their impact on consumption and savings decisions. We explore parameter values starting from 1.4, as used in Smets and Wouters (2007) and Nordhaus (2017), up to higher values common in asset pricing models. The results are shown in Panel C of Figure E.1. We find that the degree of nominal rigidities reduces the response to inflation during the transition, but is not significant enough to change the overall outcome. This finding suggests that the specific degree of nominal rigidities in the model does not play a critical role in driving the inflation dynamics associated with the transition. In contrast, the risk aversion parameter, which governs the responsiveness of aggregate demand to future interest rates, plays a much more important role in driving inflation and output during the transition. By increasing the risk aversion coefficient, the desire for consumption smoothing increases, as households prefer a more stable consumption path over time to avoid the uncertainty associated with fluctuating consumption levels. Consequently, consumption is less sensitive to real interest rates. This parameter is particularly critical for determining output during the transition, as relatively high risk aversion reduces the contractionary IS effect of monetary policy. An expansion is feasible if output is relatively inelastic to the real rate, allowing abatement expenditure to dominate.

E.4. **Macro-climate parameters.** We also investigate the sensitivity of the main variables to the macro-climate parameters. Specifically, Panel D of Figure E.1 reports the implications of varying damage parameter γ and abatement cost θ_1 on the outcome. To interpret γ, in the baseline scenario with no mitigation policy, a carbon stock of 1,700 gigatons generates an approximately 6.83 percent TFP loss. We explore damage parameters ranging from no climate damage to three time the calibrated value (approximately 1.1e-04). For the abatement parameter, this can be interpreted as the percentage of GDP spent on average to reach net zero. In our baseline simulation, it requires about 6.5 percent of GDP to decarbonize the economy, but we explore higher abatement costs of up to 13 percent of GDP. We find that inflation tends to increase in response to climate damage and abatement costs. This observation aligns with the earlier discussion on the effects of greenflation and climateflation on inflation. The implementation of carbon taxes and the impact of climate change on production costs contribute to inflationary pressures. Abatement costs are relatively more important in driving the cost of the transition, because higher abatement costs increase the marginal cost of production for

firms, which translates into more inflation through the greenflation channel discussed earlier. Similarly, an increased damage parameter boosts the climateflation terms, which deteriorates output as the real interest rates increase. The damage parameter is essential for driving output during the transition.

FIGURE E.1. Sensitivity to structural parameters

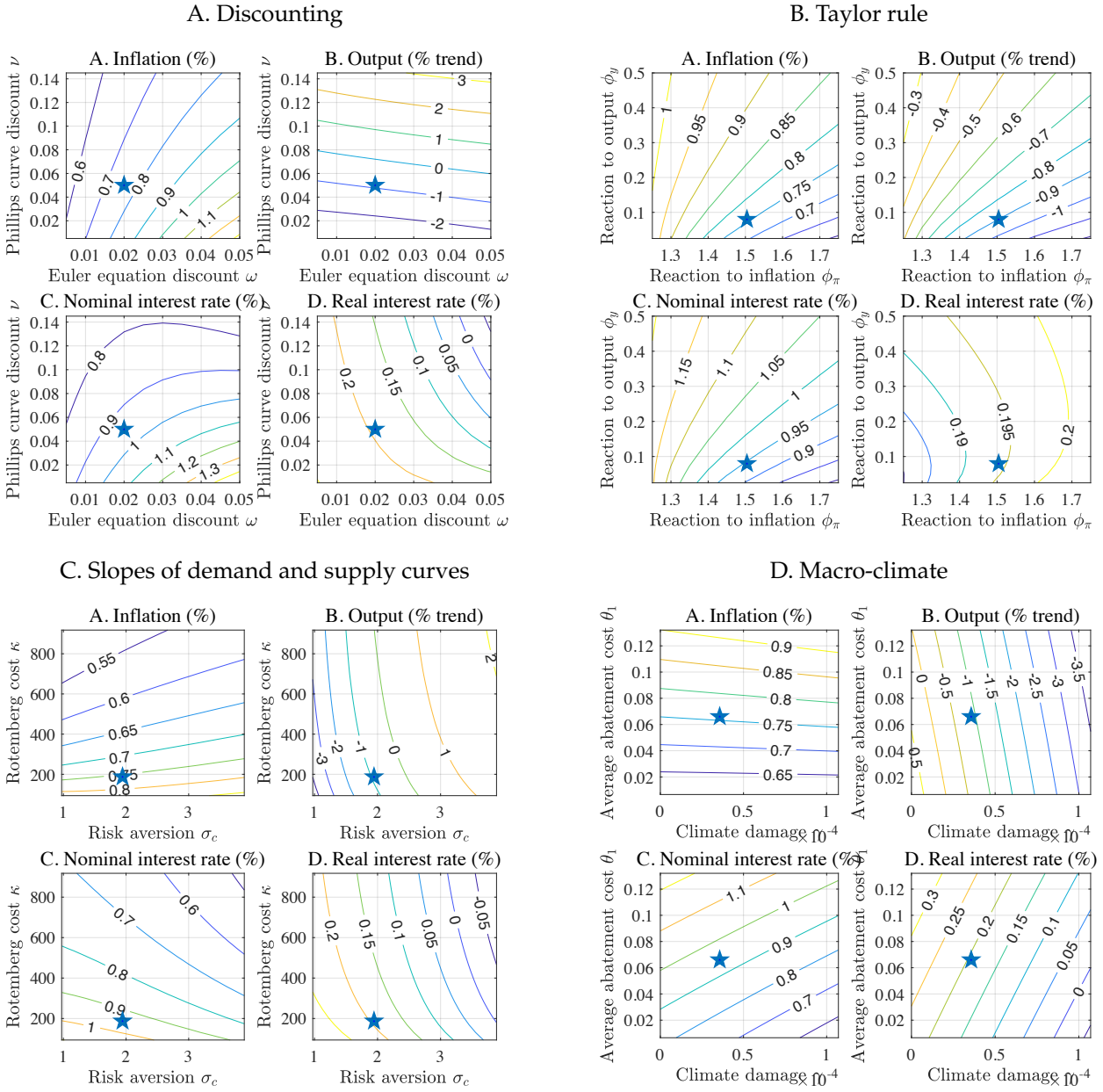

Note: This figure displays the average value between 2023Q4 and 2050Q1 for inflation, output, and nominal and real interest rates under the Paris Agreement scenario. The star represents the outcome when the parameters are set to their estimated values.